ABSTRACT

Title of Document:	OPTIMIZATION OF THE INFRARED ASPHALT REPAIR PROCESS
	Christopher William Leininger, Master of Science, 2015
Directed By:	Chair and Professor, Dr. Charles W. Schwartz, Department of Civil and Environmental Engineering

Infrared asphalt repair is an alternative technology that potentially allows for year round pavement patching that can be more durable, less expensive, and longer lasting than conventional techniques. Although infrared repair has been used for over 10 years by state and local agencies and commercial property owners in several areas of the country, some continuing resistance to this technique still remains. The principal reasons for this resistance are the largely unknown engineering properties of the patch material as compared to the native in situ pavement and the lack of standardized methods, specifications and quality assurance procedures. The following is a preliminary assessment of these engineering properties and current QA/QC procedures. A proposed specification for adoption is included in addition to recommendations for improving current practice.

OPTIMIZATION OF THE INFRARED ASPHALT REPAIR PROCESS

By

Christopher William Leininger

Thesis submitted to the Faculty of the Graduate School of the
University of Maryland, College Park, in partial fulfillment
of the requirements for the degree of
Master of Science
2015

Advisory Committee:
Dr. Charles W. Schwartz (Chair)
Dr. Dimitrios G. Goulias
Dr. Ahmet H. Aydilek

Dedication

To my friends, thank you for your support and the fond memories.

To the Professors of the Institute, thank you for the inspiration and the opportunity.

“Before I came here I was confused about this subject. Having listened to your lecture I am still confused. But on a higher level.”
-Enrico Fermi

Acknowledgements

I would like to personally acknowledge Dr. Brian Phillips for his willingness to provide me an opportunity to do research as an undergraduate, which influenced my entry into graduate school.

I would like to personally thank Dr. Charles Schwartz for his generosity in providing me a Graduate Assistantship in tough economic times. Without his support and guidance, I would not have had this opportunity to complete my graduate education.

Jay Perry, President of Pothole Pros Inc., was also instrumental for the partnership and successful completion of this study and I wish to extend my thanks to him and his work crew.

Robyn Meyers, Product Manager, at Troxler Electronic Laboratories Inc. was kind enough to allow us the use of some of their equipment, pro bono, in the completion of this study. I wish to extend my thanks to her and Troxler for their assistance.

I would also like to acknowledge Dr. Dimitrios Goulias, and Dr. Ahmet Aydilek for serving on my committee and for all their support and help.

Finally, I would like to express my appreciation to my brother, Aaron Leininger, and his roommate, Praneeth Thalla, for their friendship and assistance in performing field and laboratory work as short notice.

Table of Contents

List of Tables

List of Figures

Chapter 1: Introduction

Hot in-place asphalt recycling (HIR) is an on-site and in-place process that preserves or maintains deteriorated asphalt pavements while requiring very little new material. The HIR method is used to correct surface distresses that are not caused by problems in the base or subgrade. Of the different types of HIR methods available, Infrared Asphalt Repair (IAR) is a localized surface recycling technique. IAR is an effective remedial technique for potholes, local depressions, limited extent cracking, and other localized pavement defects. Infrared heaters are used to soften the upper portion of the pavement. The scarified upper asphalt material is then mixed with a binder rejuvenator and virgin hot mix asphalt (HMA) mixture, leveled, and compacted to grade. Figure 1 compares the edges of a traditional mill-and-fill patch vs. an infrared patch; the infrared patch has a near seamless transition to the surrounding parent pavement material and helps to prevent cold joints which are points of failure for patches.

Figure 1 Plan view of patch edges for traditional and infrared repair patches.
(a) Traditional mill-and-fill patch (b) Infrared repair patch
Source: Pothole Pros Inc.

It is the objective of this thesis to evaluate the IAR process as performed by a local Maryland company-Pothole Pros Inc., which is partner with the University of Maryland in the Maryland Industrial Partnership (MIPS) program. More specifically, the objectives of the study are as follows:

1. Evaluate and document the current IAR process and determine its strengths and weaknesses as a construction technique.
2. Investigate and confirm the integrity and engineering properties of the patch material and perform a relative comparison with the surrounding undamaged native pavement.
3. Investigate and develop construction best practices in order to ensure Quality Assurance and Quality Control (QA/QC) requirements are met. A proposed QA/QC specification is to be drawn up for adoption by the Industry.

Conclusions drawn from these analyses are presented herein. In addition, recommendations to further improve the usage of the IAR process are also presented.

This thesis is organized into eight chapters:

Chapter 1 – Introduction

States the objective of the thesis and presents a brief background to the topic of the study. It also presents the framework for the body of the thesis.

Chapter 2 – Previous Work

This chapter provides a literature review of several journal articles, technical reports, and existing QA/QC specifications. The topics reviewed include asphalt mat

heating/cooling models, studies on the IAR process, and studies on more general Recycled Asphalt Pavement (RAP) usage.

Chapter 3 – Infrared Asphalt Repair Process in Pavements

This chapter illustrates the current IAR process as performed by Pothole Pros Inc. It presents a walk thru of the process and a discussion of the current level of QA/QC applied to projects.

Chapter 4 – Field Evaluation of Asphalt Heating

This chapter discusses the experimental setup, equipment, and testing done to investigate the heating that the asphalt undergoes from the patching process. A brief discussion of environmental factors that influence the rate of heating will be discussed.

Chapter 5 – Numerical Model of Asphalt Heating

In this chapter the asphalt heating investigated previously in the field will be modeled with both a finite difference method and a finite element method. Key inputs to these analyses are the thermophysical properties of asphalt and other heating parameters. The two models are compared and commented upon.

The predicted asphalt heating response from the numerical model is compared to the field measurements of the asphalt heating. Insights from this process are discussed as well as limitations of the model.

Chapter 6 – Laboratory Analysis of Asphalt Patches

Laboratory analysis of the patch material is presented here. Investigation of the bulk specific gravity and the indirect tensile strength of specimens give insight into the importance of the compactive effort, application rate of the asphalt rejuvenator, and different heating schemes.

Chapter 7: Conclusions and Lessons Learned

This chapter presents a summary of conclusions, lessons learned, and recommendations for future studies involving IAR technology in pavements.

Chapter 2: Previous Work

A literature review of several journal articles, technical reports, and existing QA/QC specifications was conducted. Though a number of other literature pieces were reviewed only the most pertinent are discussed here. The topics reviewed include studies on the IAR process, asphalt mat heating/cooling models, and studies on more general Recycled Asphalt Pavement (RAP) usage.

2.1 Nazzal, Kim and Abbas 2014

In 2014 Nazzal (Nazzal et al. 2014) and others conducted a study for the Ohio Department of Transportation. The objective of this study was to investigate the performance and cost effectiveness of IAR methods compared with typically used throw-and-roll and spray injection pothole repair methods. They conducted a national survey that investigated the performance and satisfaction levels of the users of IAR. In addition to this they also installed over 60 patches on a section of Interstate 480 (I-480) and monitored them for long term survivability and performance. This is important, as the long term survivability and performance results complements the present research that is more focused on the immediate properties of the patch material.

Nazzal et al.'s most significant findings are that IAR has lower productivity as opposed to throw-and-roll and spray injection, mostly due to the time required to heat the pavement. In general they discovered that most of the deterioration in the patches installed using the different methods occurred soon after the patch was placed, typically within the first month of installation. If the patch could survive past this mark then its

integrity was generally assured. It was found that the infrared patches had significantly better performance from a survivability perspective than those installed using the two other patching methods. The main distress they discovered for infrared patches was susceptibility to raveling, as opposed to dishing for the throw and roll and spray injection patches. This is indicative of a lack of proper rejuvenator application as opposed to compaction problems, as suggested by the dishing. It is noteworthy that the IAR patching performed by Nazzal et al. did not include the use of rejuvenators, which are typically used in HIR and RAP applications.

The results from Nazzal et al.'s survivability analysis also indicated that the patches installed using IAR had much longer lives than those installed using the other two methods and generally outlasted the 14 month study period. In summary, Nazzal et al. found IAR to be an efficient and cost effective method for patching certain types of potholes as well as performing other localized pavement repairs.

2.2 US Army Corp of Engineers

The US Army Corp of Engineers (Carruth & Mejías-Santiago, et al., 2013) investigated HIR technology that utilizes RAP rather than virgin HMA for application in sustainable remote and isolated airfield repair. They investigated the use of rejuvenator products and infrared heaters and then evaluated the patches with simulated F-15 fighter jet traffic.

Asphalt rejuvenators are petroleum distillates that are applied to pavements in order to preserve and maintain them by reversing asphalt binder oxidation. Asphalt binders are fractionated into two main subdivisions, asphaltenes and maltenes, which

consist of different hydrocarbon bases (Boyer, 2000). As binders oxidize and weather, maltenes degrade into asphaltenes that result in dry and brittle pavements that are prone to cracking. Rejuvenators typically contain high portions of maltenes.

Many rejuvenators are proprietary, making it difficult to offer a good generic description beyond ASTM D4552. However, many rejuvenators contain these maltenes. Heating of asphalt binder can also prematurely oxidize the binder, which is an important consideration for IAR methods. The introduction of maltenes from rejuvenators will rebalance the maltenes-aphaltene ratio and soften the older asphalt. Rejuvenators will retard the loss of surface fines and reduce the formation of additional cracks; however, they will also reduce pavement skid resistance for up to one year (Army and Air Force, 1988) and overuse can result in soft pavement.

The Corp of Engineers in the course of their research investigated the effect of asphalt rejuvenator content on the rheological properties of the recycled materials and determined an optimum dosage by weight of the recycled mix with respect to the dynamic modulus and rutting depth, Figure 2. They investigated four commercially available asphalt rejuvenators and found that the most significant factor affecting dosage was the rejuvenator-water mixing ratio (Carruth & Mejías-Santiago, et al 2014).

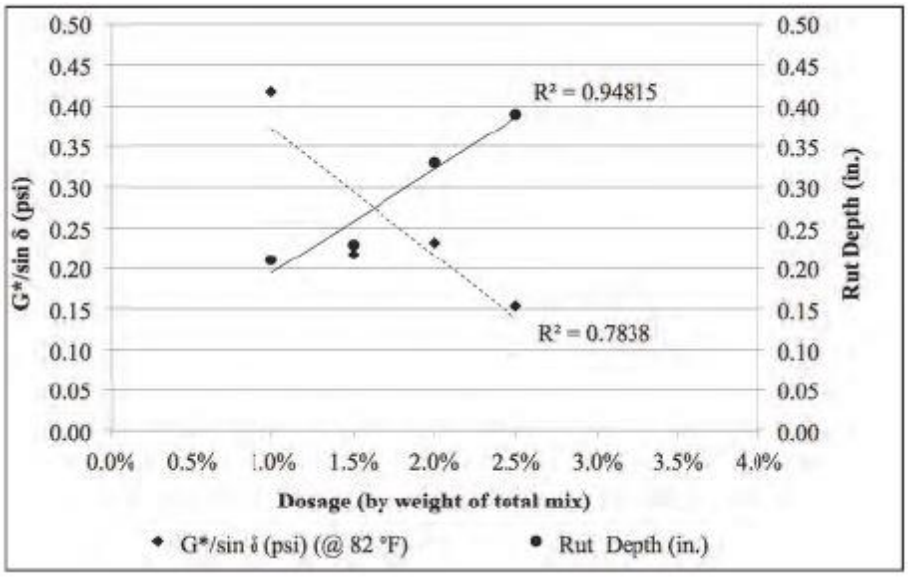

Figure 2 USACE Cyclogen LE Rejuvenator Optimum Dosage (Carruth & Mejías-Santiago, et al 2014).

Importantly, Carruth & Mejías-Santiago et al. studied the elastic properties of the binder and conducted oxidation tests of the asphalt binder after being exposed to both electric and propane heaters for 3, 4, and 5 hours. They found that even after such a long heating time of 5 hours only the top ½ inch to 1 inch of the pavement prematurely oxidizes and stiffens, forming a crust as seen in Figure 3. The stiffening of the pavement due to premature oxidation makes them more susceptible to cracking and raveling. Typically, the top ¼ inch to ½ inch of material is removed after heating in IAR. Carruth & Mejías-Santiago et al.'s research provides evidence that this is a best practice and should continue to be implemented in a consistent manner.

Figure 3 USACE Asphalt ½" Crust from Oxidation Tests (Carruth & Mejías-Santiago, et al 2014).

2.3 Freeman

Freeman and Epps (2012) published a report for the Texas Department of Transportation and the Federal Highway Administration that detailed the use of an IAR method performed by HeatWurx^{TM} that consists of heating the pavement surface, scarifying the surface, blending old millings from past projects in with the existing material, and then compacting the material.

They discovered concerns with the HeatWurx^{TM} process that seemed to stem from a lack of consistent QA/QC procedures implemented by the repair crew. They noted that the heating duration was arbitrarily decided by the crew supervisor and that the amount of rejuvenator was estimated visually by the crew. This led to a measured temperature at compaction of 150^{o}F rather than the typical 200^{o}F temperature. The authors believed that this and other factors such as excess rejuvenator and low air voids were responsible for a number of the test patches failing at one of the test sites due to

shoving and rutting (Freeman and Epps, 2012). On one test patch they took two cores and evaluated the bulk density, resilient modulus, and indirect tensile strength. Table 1 provides a summary of these test results. It is seen that the cored patch has very poor engineering properties compared to the original surrounding pavement.

Table 1 Summary of laboratory results for IAR patching (Freeman and Epps, 2012).

Sample	Bulk Density, lb/ft^3	Air Voids, %	Resilient Modulus @ 39.2°F, ksi	Resilient Modulus @ 77°F, ksi	Indirect Tensile Str. @ 77°F, psi
Original Pavement	143.0	7.4	2686	1512	187
Core 1	133.5	10.9	221	134	17.0
Core 2	137.8	8.1	489	172	26.2

Freeman and Epps' conclusion is that the IAR process as performed by HeatWurk™ might be an acceptable alternative to pothole patching, especially in remote areas, but it is not well suited to urban areas where other options are available. In the end, Freeman and Epps' study can be taken as a cautionary tale about the importance of consistent and well developed QA/QC procedures, as these can have a tremendous impact on the performance of the patch.

2.4 Uzarowski

Uzarowski et al. (2011) performed a small study on the use of IAR methods for fixing asphalt reflective cracking in New Hamburg, Ontario. Their construction method consisted of heating the pavement surrounding the crack, scarifying the area around the crack until the crack is filled and no longer visible, adding additional virgin HMA material as needed, and then compacting. Of note is that the patches were performed in 1997 and assessed in 2010 when the street was being repaved. After 13 years these

patches had few structural defects and were in good condition. Uzarowski et al. assessed the quality of the patches via surface smoothness evaluations, and extracted cores were evaluated for density and bonding to the existing pavement. They found the materials to be well bonded with no cold joints between the patch and the existing material and that the density of the patch material was within 92-96.5% compaction (Uzarowski et al, 2011). Importantly, this study demonstrates that, with good construction practices, IAR patches can have a long life with few structural defects.

2.5 Pfieffer

Pfieffer (2010) performed an analysis of asphalt mat cooling to compare measured cooling as opposed to predictions from a finite difference model. This work was done with the intention of assessing and improving asphalt concrete compaction during construction. The predictive model developed by Pfieffer was extended in the present study to an asphalt mat heating model by adding a radiation forcing function to the finite difference formulation. This forcing term models the effects of the heat flux from the infrared heater.

This model was developed based upon the principles of one-dimensional heat flow within a homogenous solid (conduction), which is described by the following partial differential equation (PDE):

$$\frac{\partial T}{\partial t} = \alpha \frac{\partial^2 T}{\partial y^2} \tag{1}$$

in which T is temperature, t is time, y is depth, and α is the thermal diffusivity, or the ability of a material to conduct thermal energy in relation to its ability to store thermal energy. Thermal diffusivity is defined as:

$$\alpha = \frac{k}{\rho * C_p} \quad \left(\frac{ft^2}{hr}\right) \tag{2}$$

in which k is thermal conductivity, ρ is material density, and C_p is specific heat. The heat flow can be depicted as in Figure 4, where the infrared heater is characterized as a radiation forcing function going into the slab (the slab also radiates heat out away from itself). Conduction transfers energy from the high temperature surface to lower temperature areas of the overlay, and convection transfers heat between the solid pavement and the liquid or gas at the surface.

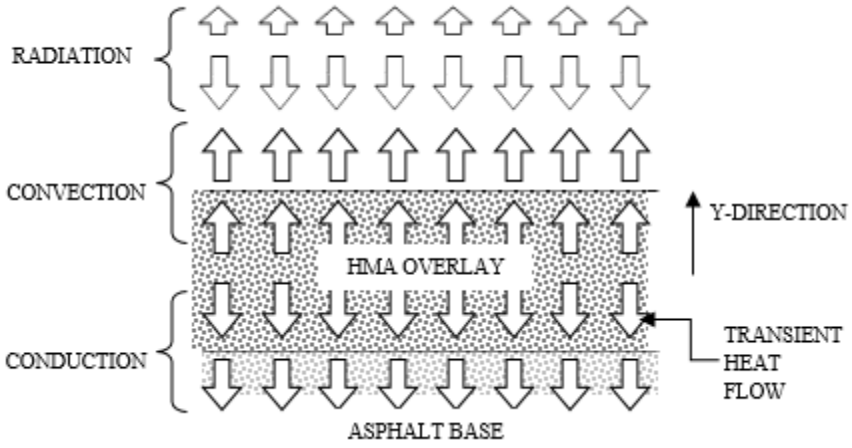

Figure 4 Asphalt overlay depicting heat flow during infrared heating

The heat transfer between the asphalt slab and the surrounding environment due to convection is described by Newton's law of cooling:

$$Q_c = hA[T_A - T_{air}] \tag{3}$$

in which Q_c is the heat flux due to convection, h is the convection coefficient, A is the slab surface area, and T_{air} is the temperature of the ambient atmosphere.

The process through which the asphalt slab is heated is via radiative heat transfer. Radiation is a highly nonlinear process, with the heat transfer calculated as follows:

$$Q_{rad} = \sigma F A[\varepsilon_H T_H^4 - \varepsilon_A T_A^4] \tag{4}$$

in which Q_{rad} is the heat flux due to the radiative heating, σ is the Sefan-Boltzman constant, F is the view factor, A is the surface area, ε_H is the emissivity of the heater and ε_A is that of the asphalt, and T_H is the temperature of the heating element and T_A that of the asphalt. This represents the net heat being sent to the slab by the infrared heater less the heat the slab is shedding via radiation to the surrounding environment.

2.5.1 View Factor

The view factor, F, is a ratio of the amount of radiation received by one radiating surface from another and is a function of geometry. In this case the infrared heater radiating to the asphalt slab can be approximated as a series of cylinders radiating to a flat plate (Labeas, 2008):

$$F = 1 - \left[1 - \left(\frac{D}{S}\right)^2\right]^{\frac{1}{2}} + \frac{D}{S}\tan^{-1}\left(\frac{(S^2 - D^2)}{D^2}\right)^{\frac{1}{2}} \tag{5}$$

in which D is the IR heater diameter, and S is the distance between the cylinders of the infrared heater. This view factor calculation is technically valid for an infinite extent of cylinders above an infinite mat, as illustrated in Figure 5. However, the ratio of the patch size to the area of the infrared heater used by Pothole Pros is generally large enough that this is taken as a valid approximation, Figure 6.

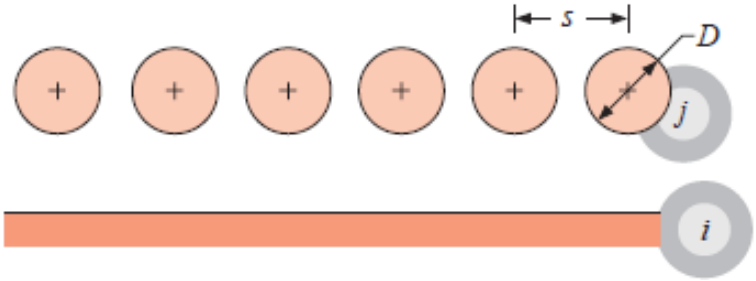

Figure 5 Infinite extent of cylinders and mat radiating. S is the spacing between cylinders and D is the diameter of the cylinders. (F. Incropera, 7th Ed.)

Figure 6 Pothole Pros Inc. infrared heater. Note the cylinder shaped heating units. The whole heater is 10'x7' but if desired only half can be turned on for a 5'x7' heat.

2.5.2 Thermophysical Properties and Other Parameters

Pfieffer conducted an extensive literature review which spanned the last 50 years of research on asphalt mat cooling. He gathered an extensive compilation of typical values for the thermophysical properties of asphalt concrete and used these to conduct a parameter sensitivity analysis that resulted in the selection of the following values for the asphalt material, Table 2. These values served as the basis for the analyses in the present study.

Table 2 Values of thermophysical properties of the asphalt used by Pfieffer in his finite difference model (Pfieffer, 2010).

Property	Units	Symbol	Used
Thermal conductivity	BTU/ft-hr-°F	k	0.64
Thermal diffusivity	ft^2/hr	α	0.0213
Convective heat transfer coefficient	Dimensionless	h	1.30
Thermal emissivity	Dimensionless	ε	0.95

2.7 Existing QA/QC Specifications

Specifications for HIR are available at the national level from the FHWA and the U.S. Army Corps of Engineers and at the state level for AZ, CA, FL, NY, and TX, Some contractor-developed specifications were also identified. However, for IAR proper there are far fewer specifications available. A search for existing specifications for infrared pavement repair found guidelines/specifications from Somerset County NJ, Canon City CO, and the AASHTO Technology Implementation Group. The similarities and differences among these specifications are summarized in Figure 8. These existing

specifications have been utilized as appropriate in the development of the proposed specifications from this study.

While these existing specifications are often in agreement, none of the three seem to address the IAR process in its most general form or incorporate up to date research from the literature on best practices. Most of the suggestions and requirements are based upon typical best practices for conventional asphalt construction techniques. The IAR-specific construction practices mandated in the specifications are often difficult to assess in the field. For instance the specifications all mandate proper compaction but do not specify how to assess this in the field either via number of passes with a roller (method specification) or via use of a nuclear or non-nuclear density gage (result specification). The Canon City and Somerset requirements for rejuvenating agent do not specify the amount to be used. This can lead to problems with the patch, as too much rejuvenator can result in a soft and rut susceptible pavement while too little can result in brittle and crack prone patches.

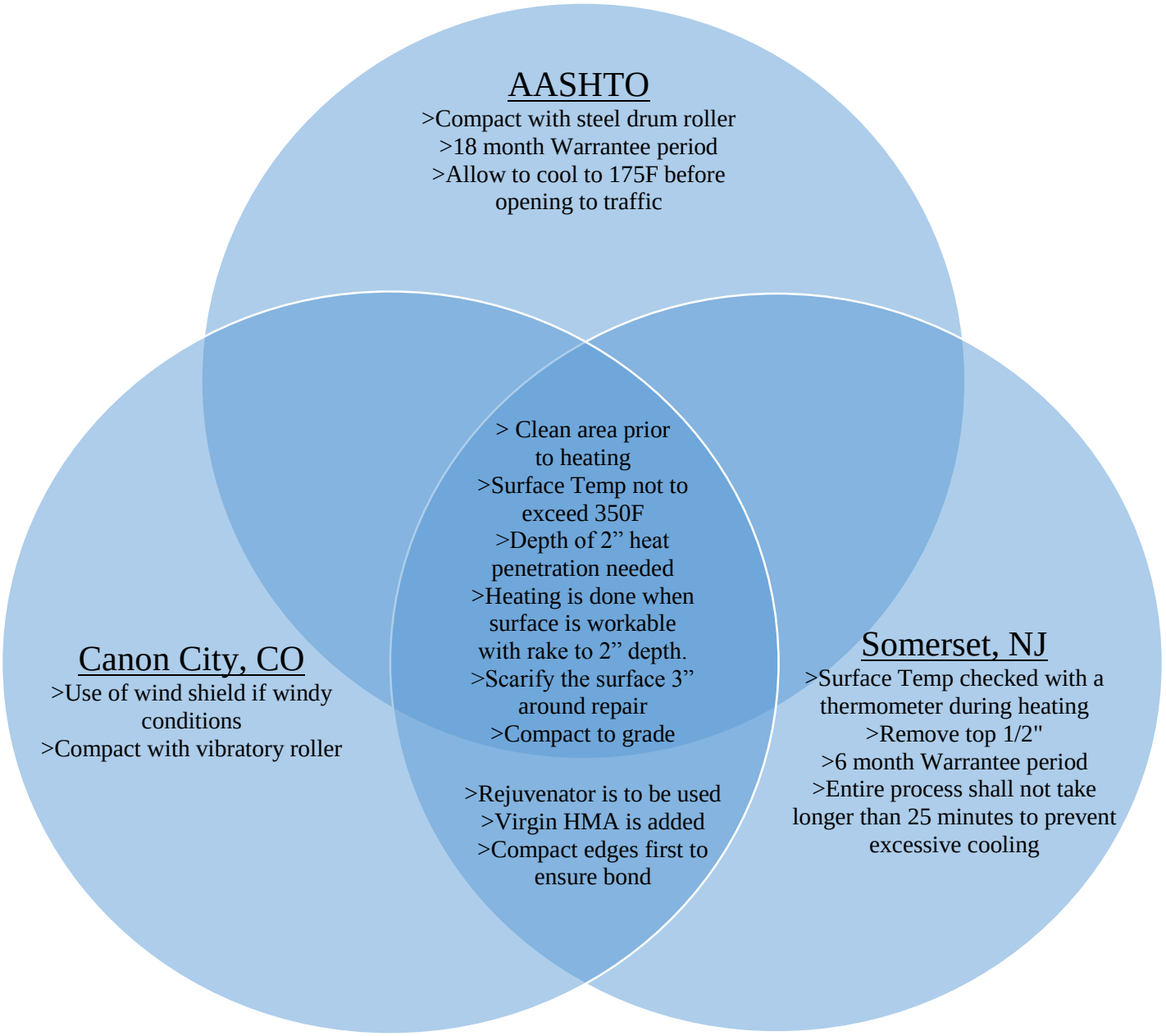

Figure 7 Comparison of the three specification for IAR construction practices.

Chapter 3: Infrared Repair Process in Pavements

3.1 Walk Thru of Process

The current process utilized by Pothole Pros Inc. has been established thru adherence to equipment manufacturers advice combined with conventional industry knowledge and standards. Their techniques have been further refined via empirical adoption of techniques that have contributed to pavement repair success and customer satisfaction. The 10 step process is outlined below and illustrated in Figure 8.

1. Owner and Contractor identify the locations to be patched and Contractor outlines the proposed repair method to their crew.
2. Contractor's crew comes out to site with Pavement Restoration Vehicle (PRV) that contains fresh HMA picked up from a local HMA plant.
3. The damaged pavement is brushed or air blown to remove dirt and excess moisture.
4. The infrared heater is ignited and is centered over the patch at a height of 12 inches. The heater ultimately reaches a temperature of 1200 degrees F and is held over the patch for 8-14 minutes based upon the crew's subjective assessment of the pavement age, weather, and other existing conditions.
5. The crew assesses that the pavement has been effectively heated to a depth of 2 inches by checking with a steel rake or shovel that the existing asphalt has been made sufficiently workable.

6. The top 1/2 inch of existing pavement is scrapped off and removed in order to remove potentially charred asphalt and to make room for virgin HMA that will be placed. The remaining pavement surface is scarified.
7. Cyclogen LE is sprayed on the exposed and scarified hot pavement surface.
8. Virgin HMA is placed and luted using a steel rake or shovel.
9. A small vibratory steel drum compactor is used to compact the surface to existing grade. Compaction begins with the edges of the patch in order to ensure a thermal bond.
10. The patch is allowed to cool before opening to traffic.

The method described above has been utilized for several years and generally creates a long lasting patch and customer satisfaction. However, the process, though refined through the trial and error and the experience of the crew, is subject to human error from new and less experienced workers, different heating rates and potential asphalt charring due to environmental factors, varying rates of asphalt rejuvenator application (ARA), and the difficulty of ensuring adequate compaction.

Figure 8 An illustration of the 10 step IAR construction process done by Pothole Pros Inc. This project took place June 4th 2014 at a project at Oxen Hill, MD.

3.2 Current QA/QC Implemented

Currently there is no codified QA/QC procedure that Pothole Pros Inc. follows as they perform their work. The work crew relies on their extensive experience and a 12 month warrantee to ensure the quality of their work.

The crew exhibits extensive field knowledge of many of the factors that influence the heating process and are cognizant of the concerns in charring asphalt. They possess an infrared thermometer that they use to ensure that the surface does not excessively char. They also use it to assess the temperature of the patch during compaction.

Their Pavement Restoration Vehicle (PRV) is equipped with a HMA hotbox that keeps fresh virgin HMA at temperatures between 250-325ºF. They typically use a 9.5 mm PG 64-22 virgin mix that is picked up from a Maryland Department of Transportation approved local plant the morning before a project.

Compaction is performed with a Vibco GR-3200 vibratory compactor. This is capable of applying 3200 lbs. of dynamic force at a frequency of 5400 vibrations per minute. Though the crew does not measure the number of passes performed per patch, it was observed in the field that they typically performed around 20 passes per 5'x7' patch, beginning on the edges in order to ensure good patch bonding to the surrounding existing pavement.

The crew uses a hand pump sprayer to apply the Cyclogen® LE rejuvenator to the scarified heated surface and around the edges of the existing pavement prior to the addition of the virgin HMA, Figure 9. This ensures that maltenes are reintroduced to

the aged existing pavement. The Cyclogen is a dark brown color that is visible against the asphalt background. This allows the crew to visually assess the coverage of the applied rejuvenator prior to it soaking into the asphalt. However, they do not measure the amount applied and typically do not evenly spray the rejuvenator across the patch with a spray nozzle. This stems from equipment maintenance issues. The Cyclogen rejuvenator at the end of the day dries and gums up the spray nozzle requiring soaking in a solvent (diesel fuel) overnight. The diesel fuel has the unfortunate side effect of degrading the rubber gaskets used in the pump sprayer.

Figure 9 Application of Cyclogen asphalt rejuvenator (brown liquid) to the patch without a spray nozzle.

Chapter 4: Field Evaluation of Asphalt Heating

4.1 Experimental Setup

An experimental setup was developed for measuring temperature at depth in an asphalt slab. This was done in order to assess the heating procedure and gain greater understanding of the temperature within the pavement during infrared heating from the surface. A 4 channel handheld data logger thermometer (Omega® part HH374) and high temperature insulated thermocouples (Omega® part XC-20-K-72) were utilized to measure the temperature at a depth of 1.0 inch, 1.5 inch, 2.0 inch, and at the pavement surface.

4.1.1 Testing Procedures

Multiple test sites, including several on the University of Maryland's campus as shown in Figure 10, and one in Waldorf were analyzed during infrared repair jobs. Before the repair crew began work the patch was outlined and three 1/4 inch holes were drilled within 1 inch of each other near the center of the patch. The depths of the three holes were 1.0 inch, 1.5 inch, and 2 inch, as shown in Figure 11. Asphalt binder with similar thermal properties to the in-situ asphalt was heated and used to coat three thermocouples that were inserted in the drilled holes. The asphalt binder ensured that there was a firm connection between the thermocouple and the asphalt. A fourth thermocouple was placed on the surface of the asphalt to measure the surface temperature.

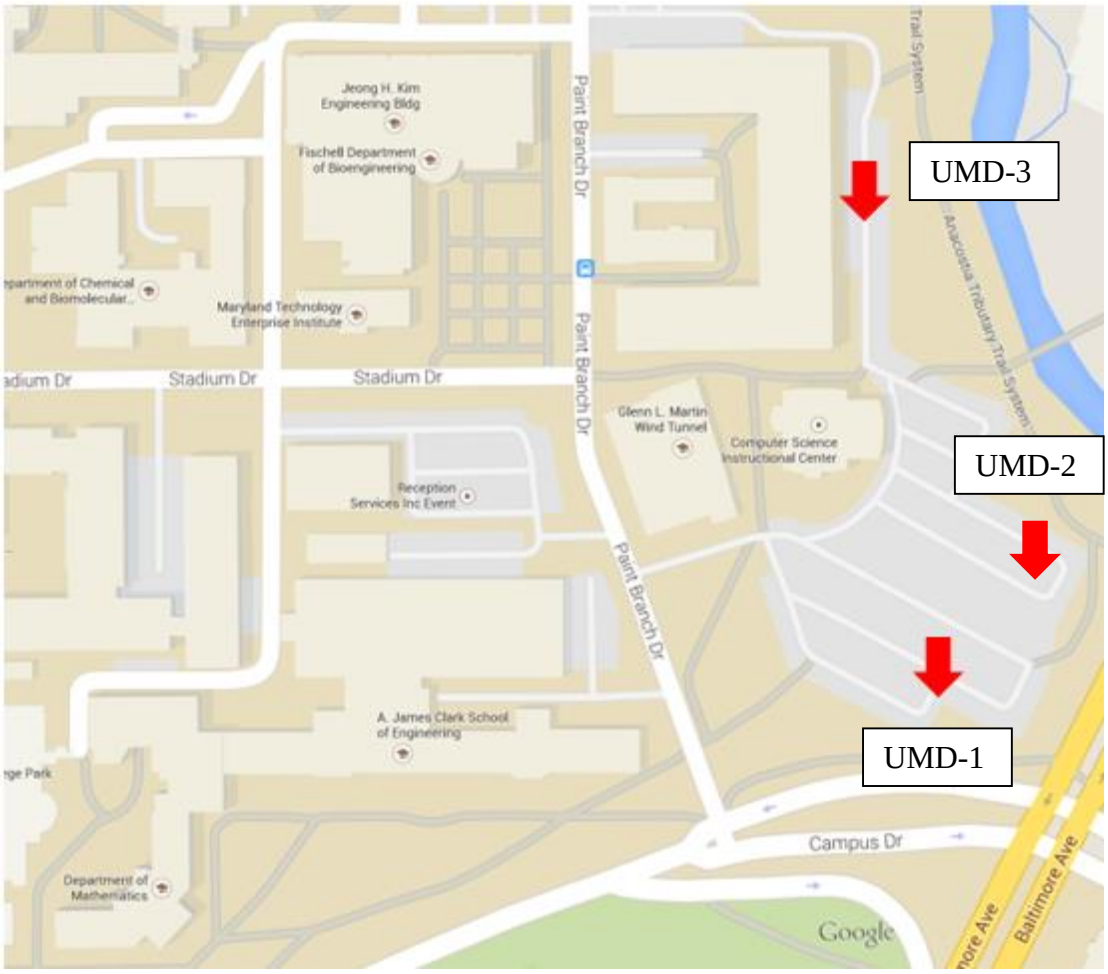

Figure 10 Location of the test sites performed at the University of Maryland. UMD-1, UMD-2 and UMD-3 are shown. Not shown are the test sites in Waldorf MD. Courtesy of Google Maps Inc.

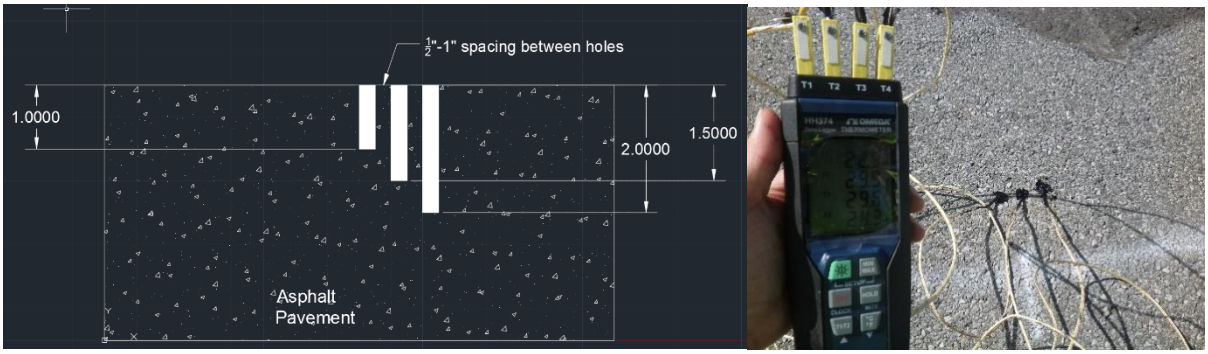

Figure 11 Experimental setup for measuring asphalt temperature within the asphalt mat. On the right is the data logger and the thermocouples installed into the asphalt slab.

During the heating phase of the repair process, the IR heater heated the slab from the surface and the data from the four thermocouples were logged on a field computer at 6 measurements per minute, Figure 12. The data was then time corrected. Key analysis points were extracted during the first 15 minutes at 0.5 minute increments and compared to the finite difference model predictions.

Figure 12 Data collection in process at UMD-1 site.

4.2 Thermocouples

A 4 channel handheld data logger thermometer (Omega® part HH374) and high temperature insulated thermocouples (Omega® part XC-20-K-72) were utilized to measure the temperature at a depth. Thermocouples work on the principle that as a metal's temperature changes so too does its electrical resistivity. This allows a data logger to record the temperature of the thermocouple as it measures the change in

resistivity. The thermocouples selected were chosen for their ability to resist and measure high temperatures (up to 2200ºF). They typically find applications in industrial kilns.

4.2.1 Variability and Reliability

The selected thermocouples were quite reliable and performed without any difficulties during the field trials. When the four thermocouples were measuring in the same environment they all measured within ± 2ºF of each other. This can be seen in Figure 13. The main issue that was discovered during the course of the data recording was that the data logging software often crashed when running under Windows 8. This resulted in two data sets being lost before a computer with Windows 7 was used with the Omega data logger.

Figure 13 The three thermocouples installed within the asphalt pavement (T2, T3, and T4) all reading within ±1.3ºF of each other.

4.3 Field Test Results

Data collected from the UMD-1 site was generally better conditioned than the readings from the Waldorf site and is reflective of a need to refine data collection techniques, particularly for the surface. One concern is that the thermocouple measuring surface temperature often is jostled loose from its taped connection and may be reading the air temperature just above the asphalt slab rather than the slab surface temperature. In future data collections, it may be advisable to drill to a 1/4 in depth in the asphalt and anchor the surface thermocouple there to see if the quality of the measured data is better.

4.4 Comparison of Heating Curves

4.4.1 Effect of Site Factors

One noteworthy finding from this study is that each in-situ pavement heats slightly differently in response to the infrared heater. This is due to a variety of factors that include the asphalt binder type, age, surface cleaning and preparation prior to heating, the ambient weather conditions, the presence of moisture in the pavement, and others. None of these factors are controllable in the field for the minor repair projects for which IAR is most suited. Nonetheless, it is important that the asphalt be sufficiently heated to a depth that ensures proper bonding between the virgin HMA and the parent material.

Chapter 5: Numerical Model of Asphalt Heating

5.1 Finite Difference Method

The Finite Difference Method (FDM) is a means for approximating the solutions to differential equations. The method is based on Taylor Series expansions for approximating derivatives.

For the general form of a second order differential equation of some field quantity, U:

$$\frac{\partial U}{\partial t} = \frac{\partial^2 U}{\partial y^2} \tag{6}$$

the transient solution may be approximated with either an explicit or implicit method. The implicit method uses a backward difference for the time derivative at time t_{j+1} and a second order central difference for the spatial derivative at location y_i. The explicit method uses a forward difference for the time derivative at time t_j and a second order central difference for spatial derivative location y_i. The implicit method is always numerically stable but is more numerically intensive. For the purposes of this project the explicit method was used, which is stable so long as the time step size is less than some critical limit, β_{HMA}.

The explicit method general formulation for Equation 6 is shown below:

$$\frac{U_{i,j+1} - U_{i,j}}{k} = \frac{U_{i+1,j} - 2U_{i,j} + U_{i-1,j}}{\frac{k}{\beta_{\mathrm{HMA}}}} \tag{7}$$

in which *i* is the space ordinate, *j* is the time ordinate, k is thermal conductivity, and β_{HMA} is a step size parameter equal to

$$\beta_{HMA} = \alpha * (\frac{\Delta t}{\Delta y^2}) \quad (8)$$

in which the time step, geometric step and thermal diffusivity are included. $U_{i,j+1}$ is the field quantity at a location i, advanced forward to time, j+1. The time integration of the explicit finite difference formulation is stable provided that parameter β_{HMA} is less than ½.

The FDM created for this project has a foundation in Pfieffer's work on asphalt mat cooling (Pfieffer, 2010), but has since been expanded. The expression for temperature moving forward in time, *j*, including boundary conditions for infrared asphalt heating is below in Equation 9 and depicted in Figure 14:

$$T_{i,j+1} = T_{i,j} + \frac{2h\alpha\Delta t}{k\Delta y}\left(T_{AIR} - T_{i,j}\right) + \frac{2\alpha\Delta t}{\Delta y^2}\left(T_{i-1,j} - T_{i,j}\right) + \frac{2a\alpha\Delta t}{k\Delta y}H_s + \ldots$$
$$\ldots \frac{2\sigma\alpha\Delta t}{k\Delta y}F\left(\varepsilon_{Heater}(T_{Heater} + 460)^4 - \varepsilon_{Asphalt}\left(T_{i,j} + 460\right)^4\right) \quad (9)$$

The $T_{i,j+1}$ is the temperature at time *j+1*, $T_{i,j}$ is it at the current time step, $\frac{2h\alpha\Delta t}{k\Delta y}\left(T_{AIR} - T_{i,j}\right)$ is the convection term, $\frac{2\alpha\Delta t}{\Delta y^2}\left(T_{i-1,j} - T_{i,j}\right)$ the conduction term, $\frac{2a\alpha\Delta t}{k\Delta y}H_s$ the solar flux term, and $\frac{2\sigma\alpha\Delta t}{k\Delta y}F\left(\varepsilon_{Heater}(T_{Heater} + 460)^4 - \varepsilon_{Asphalt}\left(T_{i,j} + 460\right)^4\right)$ is the radiation term.

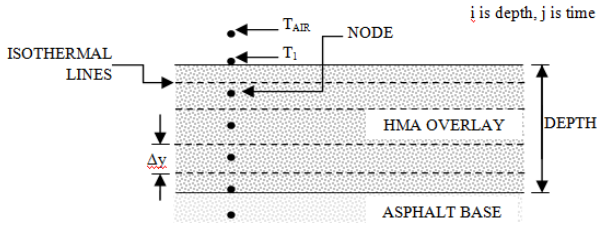

Figure 14 A pictorial representation of the finite difference method setup for asphalt mat heating. (Pfieffer, 2010).

5.2 Sensitivity Analysis

Taking the initial calculated results from the FDM, a Least Squares Error (LSE) method was applied to minimize the residual error between the Field Data and the FDM for the UMD-1 site and the Waldorf Site. Utilizing the GRG nonlinear method within Excel Solver it was possible to optimize the values of the material properties and parameters within acceptable ranges for them as specified by Pfieffer. Pre and post values can be seen for the UMD-1 site in Table 4.

Table 3 Pre and Post optimization thermophysical values for UMD 1 site.

UMD-1 Test Site			
Pre-Optimization		Post-Optimization	
h	1.3	h	1.3
H_S	0	H_S	0
a	.85	a	.85
ε_A	.95	ε_A	.9
k	.7	k	1.25
α	.0213	α	.0213
ε_H	.85	ε_H	.838
F	.248	F	.347

For F for UMD-1 was .347 and for Waldorf was .499. An average of the two is $F_{avg} = .423$ .During the parameter optimization the view factor, F, was allowed to vary the most. This reflects the approximations that are inherent at each heating site with the orientation of the heater over the pavement, the crack or pothole geometry, and other environmental factors.

5.3 Finite Element Method

5.3.1 Finite Element Formulation

Finite element methods for heat transfer begin with the same partial differential equation as seen before, here expressed in three dimensions as:

$$\rho c \frac{\partial T}{\partial t} = Q_{HG} - \left(\frac{\partial q_x}{\partial x} + \frac{\partial q_y}{\partial y} + \frac{\partial q_y}{\partial z} \right) \tag{10}$$

Where $q_x = -k \frac{\partial T}{\partial x}$ is heat flow through unit area in the x-direction and Q_{HG} is internal heat generation per unit volume. Radiative, convective, specified temperature, and specified heat flow boundary conditions may also be applied.

Utilizing shape functions N_i for the interpolation of temperature within a finite element it is possible to use the Galerkin method to rewrite the heat transfer equation, Equation 10, as:

$$\int_V \left(\frac{\partial q_x}{\partial x} + \frac{\partial q_y}{\partial y} + \frac{\partial q_y}{\partial z} - Q_{HG} + \rho c \frac{\partial T}{\partial t} \right) N_i dV = 0 \tag{11}$$

Which through further manipulation can result in the discretized finite element equations for heat transfer (Nikishkov, 2010):

$$\begin{aligned} [C]\left\{\frac{\partial T}{\partial t}\right\} + ([K_c] + [K_h] + [K_r]) * \{T\} \\ = \{R_T\} + \{R_Q\} + \{R_h\} + \{R_r\} \end{aligned} \tag{12}$$

in which $[C]$ represents material properties, $([K_c] + [K_h] + [K_r])$, the summation of the various thermal stiffness matrixes for each transfer mode (radiation, conduction,

convection), and $\{R_T\} + \{R_Q\} + \{R_h\} + \{R_r\}$ is the summation of the various loading schemes possible.

5.3.2 ANSYS Model

ANSYS is a commercial finite element software package that has a powerful suite of analysis tools. A transient 2D thermal analysis was set up within ANSYS in order to in investigate the temperature at points in the center of the slab over the course of 15 minutes (900 sec) of heating.

A 15ft wide slab 8in thick was deemed adequate for modeling an infrared heater that is 5ft wide and centered on the 15ft slab. A material was specified that mimicked that of an asphalt with the optimized parameters derived from the LSE analysis, Table 4.

The mesh was chosen to have the same resolution as the FDM, which is 0.25in elements through the thickness. ANSYS Q8 thermal mass elements are known as PLANAR77 and were chosen for the meshing. This resulted in a mesh of Q8 elements that was 720x32, for a total of 23040 elements.

It was found during the FDM analysis that the use of both the solar flux term (H_S) and convection have very small effects on the output. This would be due to the infrared heater covering the patch and blocking the incoming solar flux, and the air between the infrared heater and the asphalt heating up and minimizing the convection effects. As a result neither of these two phenomena were modeled in the FEM model.

Loads that were applied were temperature boundary conditions for the sides, radiation from the slab into space, initial slab temperature, and an incoming heat flux on a 5ft area to model the incoming radiation from the infrared heater. Figure 15 shows a screenshot of the ANSYS loading scheme. The analysis run and the applied loads are summarized in Table 4 for the UMD-1 and Waldorf test sites.

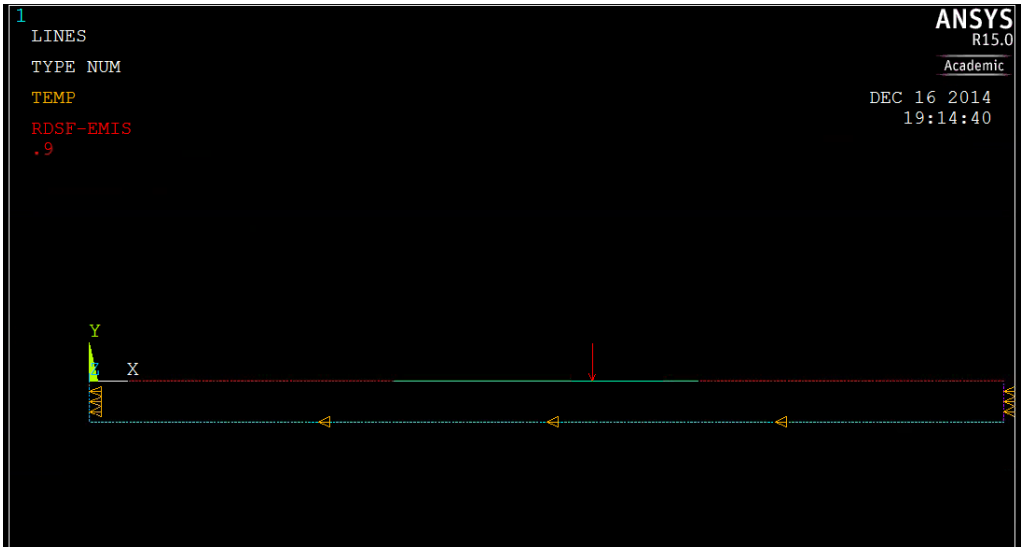

Figure 15 A depiction of the FEM model and loading on the asphalt mat.

Table 4 Summary of FEM tests performed.

	Location	Boundary Temp (°F)	Initial Asphalt Temp (F)	Q8 Element Edge Length	View Factor, F	Q_{rad} (W/m^2)
Test 1	UMD-1	100	100	0.25 in	0.423	16410
Test 2	UMD-1	100	100	0.25 in	0.347	13462
Test 3	UMD-1	100	100	0.125 in	0.423	16410
Test 4	Waldorf	80	80	0.25 in	0.423	16410
Test 5	Waldorf	80	80	0.25 in	0.499	19359

An important modeling decision was to implement the energy input from the IR heater not as a complex geometry with a high temperature (1250°F) radiating towards the slab but as a more simple applied heat flux. Taking the equation for

radiative heat transfer, Equation 4, and removing the portion that represents radiation emitted from the asphalt slab (which is modeled separately as a separate heat flux), Q_{rad} becomes:

$$\frac{Q_{rad}}{A} = \sigma F[\varepsilon_H T_H^4] \quad (13)$$

Which can be solved for with the optimized material parameters and the heater temperature. Following this approach, the heat fluxes, Q_{rad}, were determined to be $\{Q_{rad}\} = \{16410, 13462, 19359\}\ W/m^2$ for the corresponding view factors of $\{F\} = \{0.423,\ 0.347,\ 0.499\}$.

5.3.3 ANSYS Compared with Finite Difference and Selected Field Results

Of note is that Tests 3 and Test 1 from Table 4 are virtually identical except for element size and thus establish that the solution to this system is not sensitive to changes in the number of elements. It also establishes that the meshing scheme is adequate for the large aspect ratio of the geometry-15ft long by 8in thick for the asphalt slab. As a result of this comparison it was determined that the meshing and element selections were adequate, and that it is perhaps possible for fewer elements to be used and still maintain quality of the results.

Tables 5 and 6 shows a summary of the residual error analysis for the UMD-1 site the Waldorf Site. Tables 7-10 show the entirety of the results from the Least Squares Error Analysis for the UMD-1 test site. Figure 16 shows the ANSYS results from ANSYS simulated Test 3.

Results comparing the FDM and FEM analysis methods to the collected field data are consistent in that the FDM is consistently better performing in regards with total summed error residuals, Tables 5 &6. When looking through the results in Table 7-10, it is of note that for both Waldorf and UMD-1 sites at the surface and at a depth of 2", the FEM analysis performed more poorly than the FDM analysis, but at the intermediary depths of 1" and 1.5" the FEM analysis performed significantly better than the FDM. This is thought to be an indication of poorly fitted boundary conditions in the FEM model that perhaps reflects a need for mesh refinement near the pavement surface.

The collected data from the UMD-1 site is generally better behaved with less noise and atypical behavior than the Waldorf site and this explains most of the difference in the LSE values between the UMD-1 and Waldorf sites for both the FDM and FEM analysis. Figures 17 and 18 show the measured data, FDM analysis, and FEM results for the Waldorf and the UMD-1 sites specifically.

Table 5 Summary of the FDM and FEM LSE Analysis for UMD-1 Site

UMD-1 Site FDM Error vs FEM Error	
Sum of FDM Error	25,104.6
Test 1: Sum of FEM Error	39,473.4
Test 2: Sum of FEM Error	107,592.2
Test 3: Sum of FEM	39,472.2

Table 6 Summary of FDM and the FEM LSE Analysis for the Waldorf Site

Waldorf Site FDM Error vs FEM Error	
Sum of FDM Error	75,118.7
Test 4: Sum of FEM Error	37,2025.6
Test 5: Sum of FEM Error	226,264.4

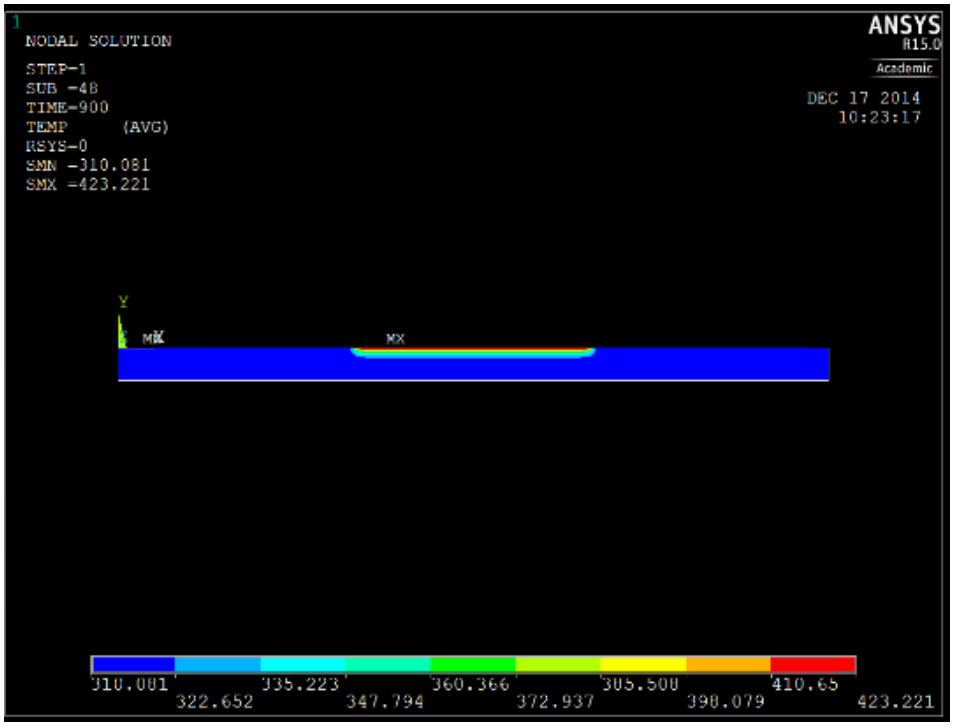

Figure 16 ANSYS results for Test 3. Note all temperatures are in degrees Kelvin.

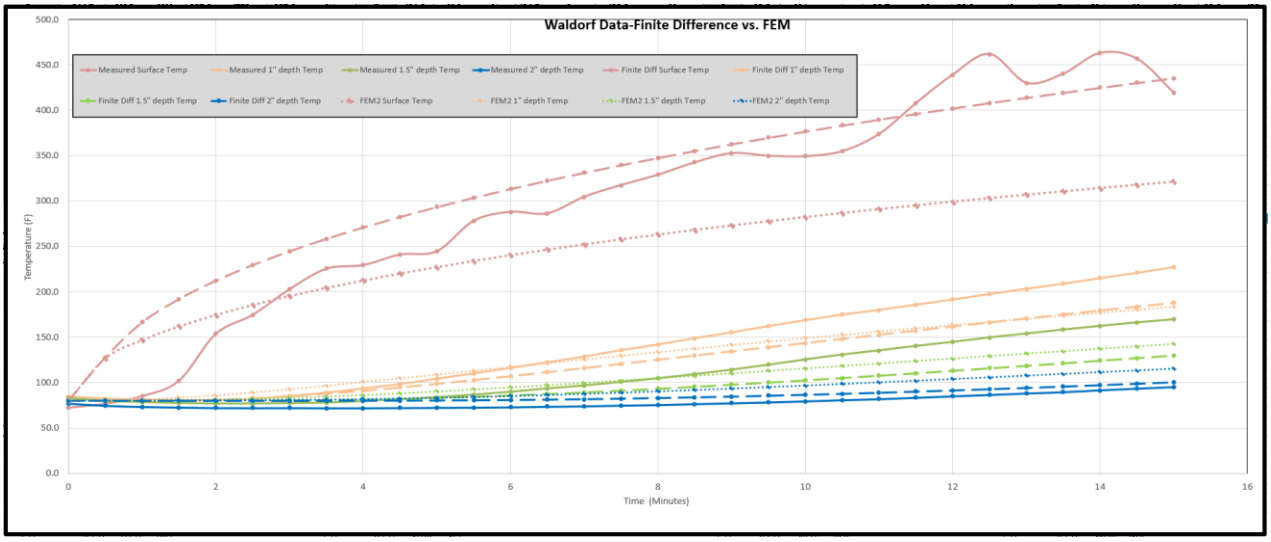

Figure 17 The measured temperature, predicted FDM, and predicted FEM at Waldorf

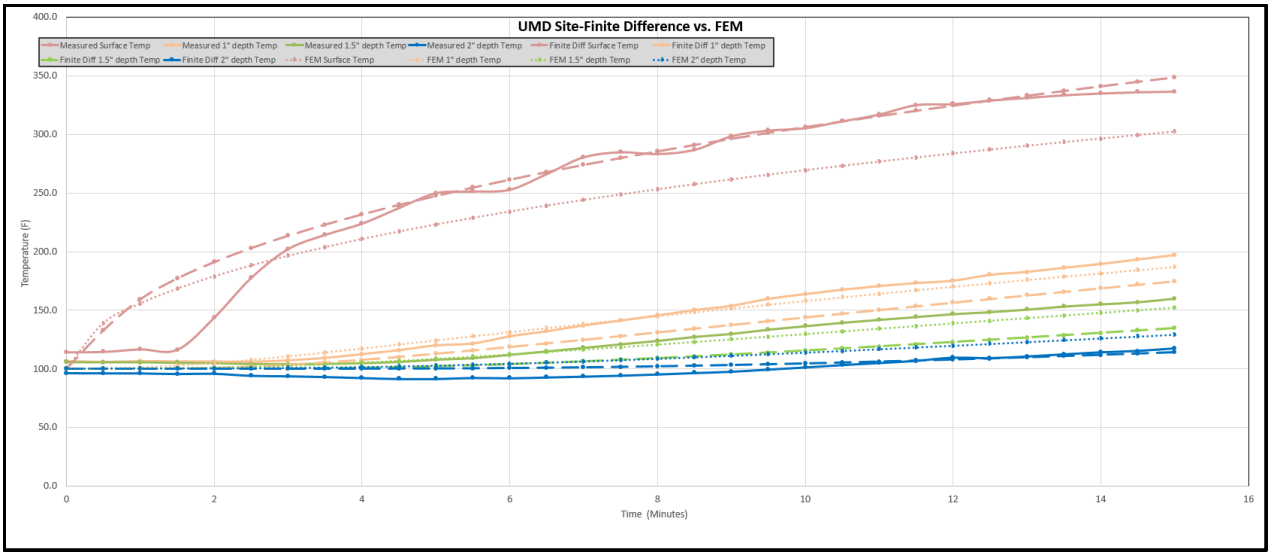

Figure 18 The measured temperature, predicted FDM, and predicted FEM at UMD-1

Table 7 LSE Analysis at the surface of the asphalt at UMD-1

UMD Site-Middle of Mat

	Surface 0"depth								
Time (min)	**Actual**	Finite Diff	FD Residual	**FEM Test1**	**FEM1 Residual**	FEM Test3	FEM3 Residual	FEM Test2	FEM2 Residual
0	**114.4**	100.0	207	**100.0**	**207**	100.0	207	**100.0**	**207**
0.5	**114.7**	132.8	328	**139.0**	**592**	139.1	594	**132.1**	**302**
1	**116.9**	159.4	1805	**155.7**	**1502**	155.6	1499	**145.7**	**831**
1.5	**116.5**	177.1	3669	**168.3**	**2681**	168.3	2682	**156.1**	**1569**
2	**143.9**	191.1	2227	**178.9**	**1222**	178.8	1221	**164.8**	**438**
2.5	**177.8**	203.0	636	**188.0**	**105**	188.0	105	**172.4**	**29**
3	**202.4**	213.6	125	**196.3**	**38**	196.2	38	**179.2**	**540**
3.5	**214.5**	223.1	74	**203.7**	**116**	203.7	116	**185.3**	**852**
4	**224.1**	231.8	60	**210.6**	**182**	210.6	182	**191.0**	**1096**
4.5	**237.4**	240.0	7	**217.0**	**417**	217.0	416	**196.3**	**1690**
5	**250.1**	247.6	6	**223.0**	**735**	223.0	735	**201.3**	**2386**
5.5	**251.5**	254.7	10	**228.6**	**523**	228.6	523	**205.9**	**2077**
6	**253.0**	261.5	72	**234.0**	**361**	234.0	361	**210.4**	**1818**
6.5	**266.4**	267.9	2	**239.1**	**747**	239.1	747	**214.6**	**2685**
7	**280.7**	274.1	44	**243.9**	**1352**	243.9	1352	**218.6**	**3855**
7.5	**285.0**	280.0	25	**248.6**	**1327**	248.6	1327	**222.5**	**3910**
8	**283.5**	285.7	5	**253.0**	**929**	253.0	929	**226.2**	**3285**
8.5	**287.0**	291.1	17	**257.3**	**881**	257.3	881	**228.1**	**3470**
9	**298.6**	296.4	5	**261.4**	**1381**	261.4	1381	**233.2**	**4279**
9.5	**303.5**	301.5	4	**265.4**	**1450**	265.4	1450	**236.5**	**4488**
10	**305.5**	306.4	1	**269.3**	**1313**	269.3	1313	**239.7**	**4326**
10.5	**311.4**	311.2	0	**273.0**	**1475**	273.0	1475	**242.8**	**4700**
11	**317.1**	315.8	2	**276.6**	**1640**	276.6	1640	**245.9**	**5075**
11.5	**325.2**	320.3	24	**280.1**	**2033**	280.1	2033	**248.8**	**5838**
12	**326.0**	324.7	2	**283.5**	**1805**	283.5	1805	**251.6**	**5528**
12.5	**329.1**	329.0	0	**286.8**	**1787**	286.8	1787	**254.4**	**5576**
13	**331.3**	333.2	3	**290.0**	**1702**	290.0	1702	**257.1**	**5501**
13.5	**333.6**	337.2	13	**293.2**	**1634**	293.2	1634	**259.8**	**5451**
14	**335.1**	341.2	37	**296.2**	**1510**	296.2	1510	**262.3**	**5294**
14.5	**336.2**	345.1	79	**299.2**	**1368**	299.2	1368	**264.9**	**5091**
15	**336.7**	348.9	149	**302.1**	**1195**	302.1	1195	**267.3**	**4815**
		sum	9637.6	**sum**	**34210.3**	sum	34210.5	**sum**	**97002.4**

Table 8 LSE Analysis for 1" depth in the asphalt at UMD-1

UMD Site-Middle of Mat

	1" depth								
Time (min)	**Actual**	Finite Diff	FD Residual	**FEM Test1**	**FEM1 Residual**	FEM Test3	FE M3	FEM Test2	FEM2 Residual
0	**106.6**	100.0	44	**100.0**	**44**	100.0	44	**100.0**	**44**
0.5	**105.9**	100.0	35	**100.4**	**31**	100.3	32	**100.2**	**32**
1	**106.5**	100.0	42	**101.1**	**30**	101.1	30	**100.9**	**31**
1.5	**106.3**	100.2	38	**102.7**	**13**	102.6	13	**102.2**	**17**
2	**106.2**	100.8	30	**104.9**	**2**	104.8	2	**104.0**	**5**
2.5	**106.0**	101.8	17	**107.6**	**2**	107.5	2	**106.2**	**0**
3	**107.2**	103.4	15	**110.6**	**11**	110.6	11	**108.7**	**2**
3.5	**109.3**	105.3	16	**113.8**	**20**	113.8	20	**111.4**	**4**
4	**112.5**	107.6	24	**117.2**	**22**	117.2	22	**114.1**	**3**
4.5	**115.9**	110.1	34	**120.6**	**23**	120.6	23	**117.0**	**1**
5	**120.0**	112.8	52	**124.1**	**17**	124.1	17	**119.9**	**0**
5.5	**121.6**	115.7	35	**127.6**	**37**	127.6	37	**122.8**	**1**
6	**127.7**	118.6	82	**131.1**	**12**	131.1	12	**125.6**	**4**
6.5	**132.0**	121.7	106	**134.6**	**7**	134.6	7	**128.5**	**12**
7	**137.0**	124.8	149	**138.1**	**1**	138.1	1	**131.3**	**32**
7.5	**141.1**	128.0	173	**141.5**	**0**	141.5	0	**134.1**	**48**
8	**145.5**	131.1	206	**144.8**	**0**	144.8	0	**136.9**	**74**
8.5	**150.1**	134.3	248	**148.1**	**4**	148.1	4	**138.4**	**138**
9	**153.7**	137.5	261	**151.4**	**5**	151.4	5	**142.3**	**129**
9.5	**159.7**	140.8	359	**154.6**	**26**	154.6	26	**145.0**	**216**
10	**163.7**	143.9	390	**157.8**	**35**	157.8	35	**147.6**	**258**
10.5	**167.5**	147.1	415	**160.9**	**44**	160.9	43	**150.2**	**299**
11	**170.6**	150.3	412	**164.0**	**44**	164.0	44	**152.7**	**319**
11.5	**173.2**	153.5	389	**167.0**	**39**	167.0	38	**155.2**	**322**
12	**175.2**	156.6	346	**170.0**	**27**	170.0	27	**157.7**	**306**
12.5	**180.2**	159.7	419	**172.9**	**53**	172.9	53	**160.1**	**403**
13	**182.7**	162.8	395	**175.8**	**48**	175.8	48	**162.5**	**407**
13.5	**186.2**	165.9	413	**178.6**	**58**	178.6	58	**164.9**	**455**
14	**189.5**	168.9	423	**181.4**	**66**	181.4	66	**167.2**	**498**
14.5	**193.3**	171.9	456	**184.2**	**84**	184.2	84	**169.5**	**568**
15	**197.1**	174.9	491	**186.9**	**105**	186.9	105	**171.7**	**644**
		sum	6512.4	**sum**	**907.7**	sum	908.6	**sum**	**5271.3**

Table 9 LSE Analysis for 1.5” depth in the asphalt at UMD-1

UMD Site-Middle of Mat

	1.5" depth								
Time (min)	**Actual**	Finite Diff	FD Residual	**FEM Test1**	**FEM1 Residual**	FEM Test3	FE M3	FEM Test2	FEM2 Residual
0	**105.7**	100.0	32	**100.0**	**32**	100.0	32	**100.0**	**32**
0.5	**105.6**	100.0	31	**100.1**	**30**	100.1	30	**100.1**	**30**
1	**105.6**	100.0	31	**100.2**	**29**	100.2	29	**100.2**	**29**
1.5	**105.1**	100.0	26	**100.5**	**21**	100.4	22	**100.4**	**22**
2	**104.8**	100.0	23	**100.9**	**15**	100.9	15	**100.7**	**16**
2.5	**104.2**	100.1	17	**101.6**	**7**	101.6	7	**101.3**	**8**
3	**104.0**	100.2	14	**102.5**	**2**	102.5	2	**102.1**	**4**
3.5	**104.3**	100.5	15	**103.7**	**0**	103.7	0	**103.1**	**1**
4	**104.8**	100.9	15	**105.1**	**0**	105.1	0	**104.2**	**0**
4.5	**105.9**	101.5	20	**106.7**	**1**	106.7	1	**105.5**	**0**
5	**107.8**	102.2	32	**108.4**	**0**	108.4	0	**106.9**	**1**
5.5	**109.1**	103.0	37	**110.3**	**1**	110.2	1	**108.4**	**0**
6	**112.0**	104.0	64	**112.2**	**0**	112.2	0	**110.0**	**4**
6.5	**114.9**	105.1	96	**114.2**	**0**	114.2	0	**111.7**	**10**
7	**117.9**	106.4	133	**116.3**	**3**	116.3	3	**113.4**	**20**
7.5	**121.0**	107.7	177	**118.4**	**7**	118.4	7	**115.2**	**34**
8	**123.9**	109.1	219	**120.6**	**11**	120.6	11	**117.0**	**48**
8.5	**127.3**	110.6	278	**122.8**	**20**	122.8	20	**117.9**	**88**
9	**129.9**	112.2	313	**125.1**	**23**	125.1	23	**120.6**	**86**
9.5	**133.5**	113.9	386	**127.3**	**38**	127.3	38	**122.5**	**121**
10	**136.5**	115.6	438	**129.6**	**48**	129.6	48	**124.4**	**147**
10.5	**139.4**	117.3	487	**131.8**	**57**	131.8	57	**126.2**	**173**
11	**141.9**	119.1	518	**134.1**	**61**	134.1	61	**128.1**	**190**
11.5	**144.3**	121.0	544	**136.4**	**63**	136.4	63	**130.0**	**205**
12	**146.8**	122.9	573	**138.7**	**66**	138.7	66	**131.9**	**223**
12.5	**148.5**	124.8	563	**140.9**	**58**	140.9	58	**133.7**	**218**
13	**150.7**	126.7	575	**143.2**	**57**	143.2	57	**135.6**	**228**
13.5	**153.3**	128.7	607	**145.4**	**62**	145.4	62	**137.5**	**251**
14	**155.2**	130.6	603	**147.6**	**57**	147.6	57	**139.3**	**253**
14.5	**157.0**	132.6	593	**149.9**	**51**	149.9	51	**141.1**	**252**
15	**160.1**	134.7	648	**152.1**	**65**	152.1	65	**143.0**	**294**
		sum	8106.8	**sum**	**886.0**	sum	886.6	**sum**	**2989.1**

Table 10 LSE Analysis for 2" depth in the asphalt at UMD-1

UMD Site-Middle of Mat

	2" depth								
Time (min)	Actual	Finite Diff	FD Residual	FEM Test1	FEM1 Residual	FEM Test3	FEM 3	FEM Test2	FEM2 Residual
0	96.6	100.0	12	100.0	12	100.0	12	100.0	12
0.5	96.5	100.0	12	100.1	13	100.1	13	100.1	13
1	96.4	100.0	13	100.1	14	100.1	14	100.1	14
1.5	95.9	100.0	17	100.2	18	100.2	18	100.2	18
2	96.1	100.0	15	100.2	17	100.2	17	100.2	17
2.5	94.4	100.0	31	100.4	36	100.4	36	100.3	35
3	94.0	100.0	36	100.6	43	100.6	43	100.5	42
3.5	93.4	100.0	44	100.9	57	100.9	56	100.8	54
4	92.5	100.1	57	101.4	79	101.4	78	101.1	75
4.5	91.7	100.1	71	101.9	104	101.9	104	101.6	98
5	91.7	100.2	73	102.6	118	102.6	118	102.1	109
5.5	92.6	100.4	61	103.4	116	103.3	115	102.8	103
6	92.3	100.6	69	104.2	142	104.2	142	103.5	125
6.5	93.0	100.9	62	105.2	148	105.2	148	104.3	127
7	93.7	101.2	57	106.2	157	106.2	157	105.1	131
7.5	94.5	101.6	51	107.3	165	107.3	165	106.1	133
8	95.5	102.1	43	108.5	170	108.5	170	107.0	133
8.5	96.7	102.6	35	109.8	171	109.8	171	107.6	118
9	97.8	103.2	29	111.1	177	111.1	177	109.1	129
9.5	99.6	103.8	18	112.4	165	112.4	165	110.3	114
10	101.4	104.6	10	113.8	155	113.8	155	111.4	100
10.5	103.4	105.3	4	115.3	141	115.3	141	112.6	85
11	105.1	106.1	1	116.8	136	116.8	136	113.8	76
11.5	106.9	107.0	0	118.3	129	118.3	129	115.1	66
12	109.6	107.9	3	119.8	104	119.8	104	116.3	45
12.5	109.2	108.8	0	121.3	147	121.3	147	117.6	70
13	110.6	109.8	1	122.9	151	122.9	151	118.9	69
13.5	112.4	110.9	2	124.5	146	124.5	146	120.2	61
14	114.1	111.9	5	126.1	144	126.1	144	121.5	55
14.5	115.3	113.0	5	127.7	154	127.7	154	122.8	57
15	117.4	114.1	11	129.3	142	129.3	142	124.2	46
		sum	847.8	sum	3469.4	sum	3466.5	sum	2329.4

5.4 Conclusions: Finite Elements vs Finite Difference

5.4.1 Comparison

In general, the FDM method performs adequately for both accuracy and model setup/computation time for the scope of work in this heat transfer problem. The use of FEM techniques with ANSYS may perhaps be excessive given the amount of time required for model set up and computations.

However, a more rigorous application of ANSYS's FEM techniques may result in a more accurate model. The comparatively poor results of the FEM analysis is likely a result of the poorly known loading conditions from the infrared heater, which is a function of the view factor, F. Modeling the physical geometry of the IR heater in 3D and utilizing ANSYS's capabilities for modeling radiation between two surfaces (ANSYS Inc., 1998) would alleviate the uncertainty inherent in the approximating equation for the view factor, Equation 5. It would allow for a model that much better approximates the energy input into the slab from the infrared heater rather than relying on the estimates from Equation 13. This is recommended for future work.

However, there is no sense in over complicating the problem. For the purposes of recommending QA/QC procedures for infrared asphalt patching, which takes place in an uncontrolled outdoor environment, it is important to remember there are many uncontrollable variables inherent to the scenario, such as puddled water on the asphalt, high wind speeds, effects of cracks and potholes on the heating process, even the presence of shade trees. As such, an overly complex analysis is likely a waste of

resources. It would be best to model this particular heat transfer problem once in 3D in order to determine a better approximation for the view factor and apply that to the 1D finite difference method, which is easy to run and optimize.

5.4.2 Usefulness and Application of Numerical Model

The results from the finite difference asphalt heating model shows reasonable agreement with the measured temperatures, evidenced in Figures 17 and 18. Each pavement that a repair crew comes across will be slightly different and respond to the infrared heater differently. This is seen in the wide range of values for the view factor, F. A variety of factors that include the asphalt binder, age, surface cleaning and preparation prior to heating, the ambient weather conditions, the presence of moisture in the pavement, pothole geometry, heater orientation, and others are responsible for this. None of these factors is controllable in the field for the minor repair projects for which IAR is used. Nonetheless it is quite important for the asphalt to be sufficiently heated to a depth that ensures proper bonding between the virgin HMA and the parent material. And what can be seen

This model is therefore useful because it allows crews to determine how deep the heat has penetrated the asphalt. This is important as the surface of the asphalt often chars and requires removal whenever the surface temperature exceeds 350^{o}F. It is important that the then exposed surface is close to 180^{o}F for good thermal bonding to the virgin HMA.

A simulation of various heating methods using the developed finite difference model has shown that even in a 'worst-case' heating scenario, Figure 19, where the initial asphalt temperature is 100F and it is heated for 18 minutes, only ~½" of the asphalt would need to be removed due to charring (temperature exceeding 350F). This is shown in Figure 19. This study accounted for the time of heating (10min, 12min, 14min, 16min, 18min), and the initial surface temperature (40F, 60F, 80F, 100F). If the pavement was allowed to be heated for a long time, (~30 minutes) it can be demonstrated that further material will need to be removed, Figure 20. As such it is conservatively recommended that for every 100ºF above 350ºF that the pavement surface reaches an additional ½" of material should be removed in addition to the initial ¼- ½" that is recommended.

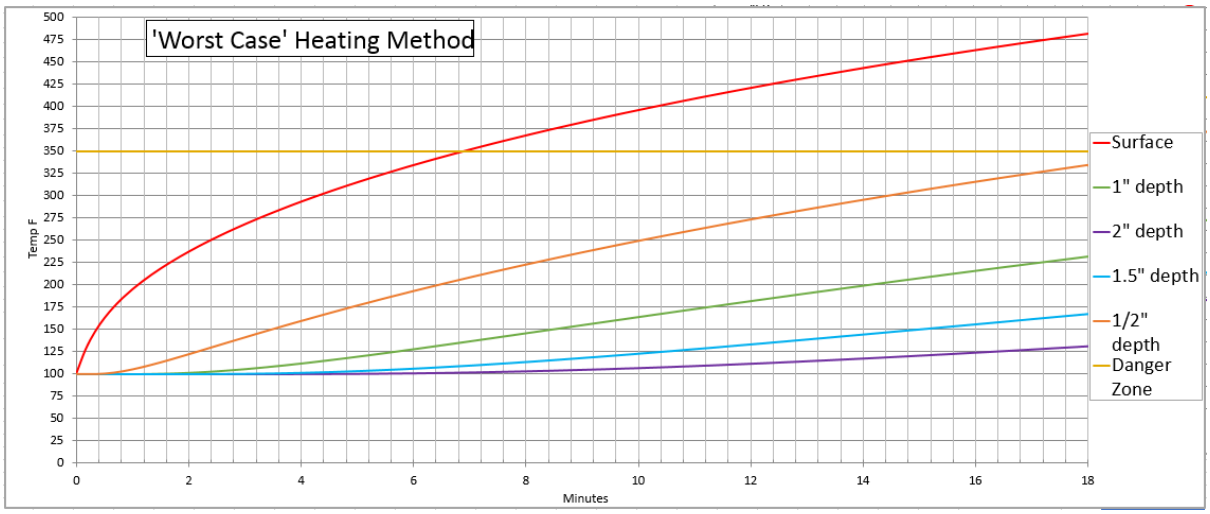

Figure 19 An example of a design chart for the amount of asphalt to remove based on the heating methods

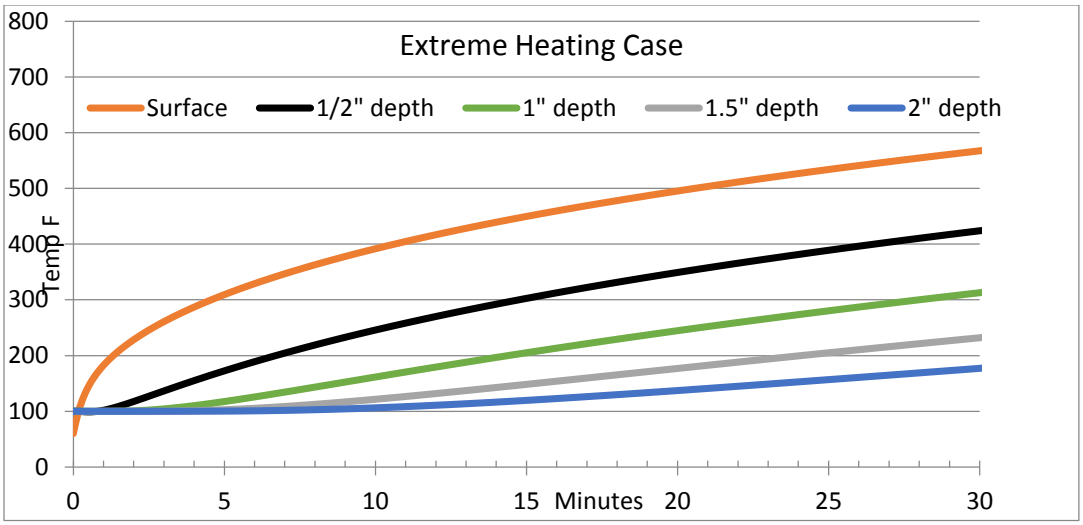

Figure 20 Extreme Heating Case

A two-stage heating scheme has also been developed in order to facilitate heat penetration deeper into the asphalt mat. This involves heating the asphalt per usual, scraping off the charred surface (either ½" or 1" of removed material) and then reheating the exposed surface for a brief period (2min, 4min, or 6min) before adding the virgin HMA. This method is meant to ensure the parent material and the virgin HMA have similar temperatures during compaction in order to get a blending effect that binds the two layers together. This is seen in Figure 21.

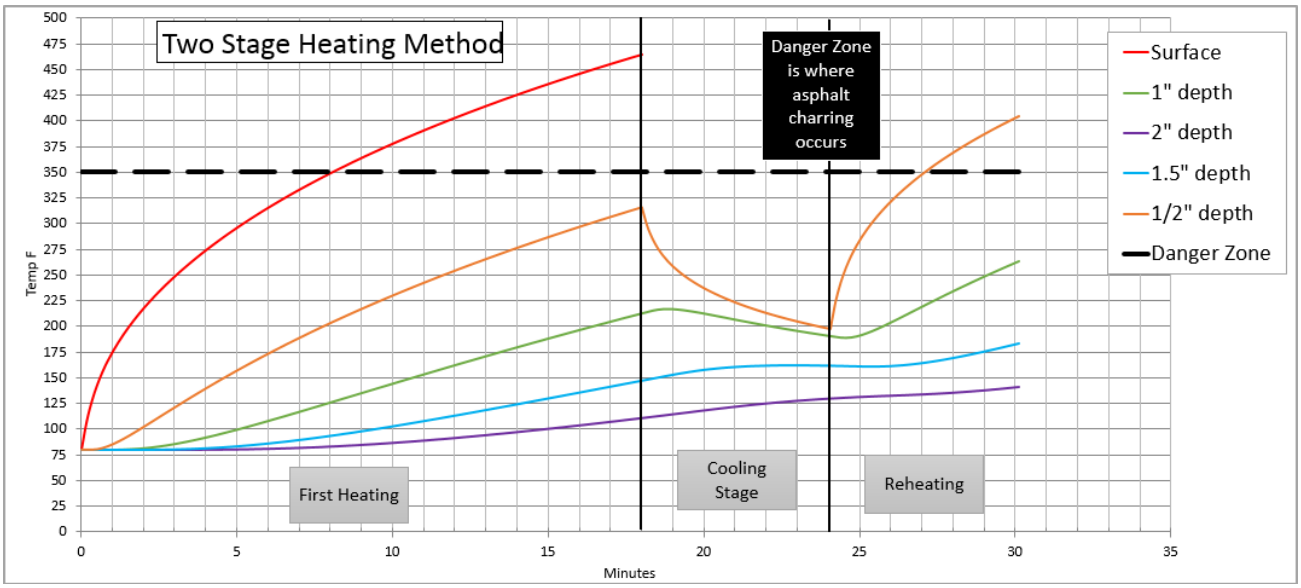

Figure 21 Two Stage Heating Scheme. The top half inch is removed after the first heating stage and the ½" depth becomes the new de facto 'surface' exposed to heating. Here the cooling period is 6 minutes and the reheating stage is 6 minutes.

Chapter 6: Laboratory Analysis of Asphalt Patches

6.1 Experimental Setup and Phase-1 Testing

One of the main goals of this project was to evaluate the material properties of the patch material that are directly impacted by construction QA/QC. The researcher shadowed the work crew and witnessed a project before working with Pothole Pros to decide on a course of action. Then, several patches were performed for preliminary Phase-1 assessment. Two patches were made in Waldorf, MD, one of which was evaluated 9 months after it had been placed (Waldorf-New and Waldorf-Old). Two additional patches were made on the University of Maryland campus (UMD-1 and UMD-2). In addition, a traditional full depth saw cut and removal and replacement patch was performed at the Waldorf site to provide a comparison with a more conventional repair technique. These patches were assessed for bulk density and indirect tensile strength and were compared against the behavior of the existing (in-situ) pavement, the existing pavement that though not part of the patch was heated by the infrared heater (In-situ heated pavement), and along the joint interface of the patch and in-situ material (Joint), Figure 22.

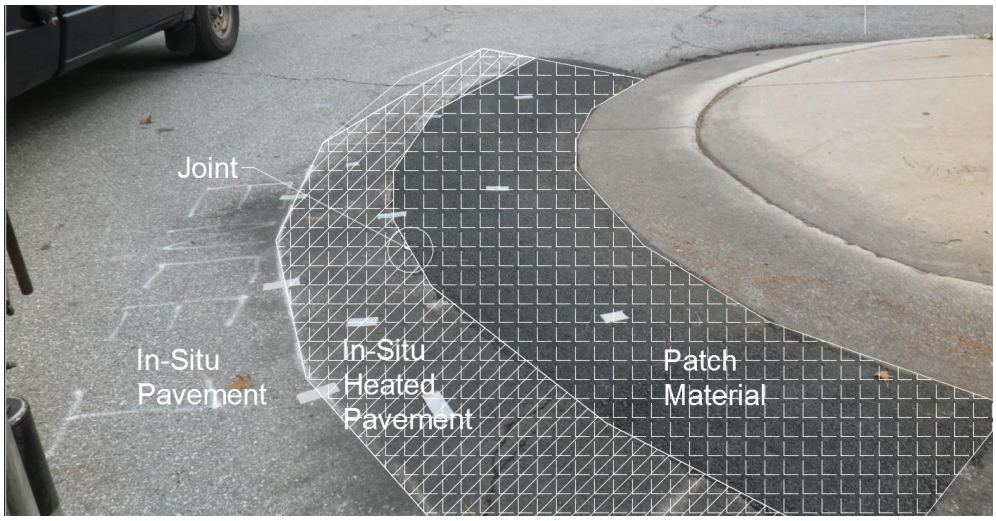

Figure 22 Details of the preliminary asphalt core sampling scheme for the UMD-1, UMD-2, and Waldorf-old/new test sites.

The results from this Phase-1 assessment are shown below in Tables 11-13.

Table 11 Summary of Results from Waldorf Site

Waldorf Site					
	Average Bulk Density	Avg. Dry ITT (psi)	Number of Specimens	Standard Deviation	Variance
In-situ Pavement	2.33	220.4	3	22.6	510
Waldorf-Old (9 months)	2.24	143.1	3	6.4	40.5
Waldorf-New	2.20	105.8	2	4.9	23.8
Saw-cut Patch	2.29	110.5	2	13.1	179.4

Table 12 Summary of Results from UMD-1

UMD-1					
	Average Bulk Density	Avg. Dry ITT (psi)	Number of Specimens	Standard Deviation	Variance
In-situ Pavement	2.42	177.1	3	32.5	1053
Heated in-situ Pavement	Na	180.9	3	7.3	53.6
New Patch	2.34	165.7	3	39.4	1548
Joint	Na	177.7	3	14.3	204

Table 13 Summary of Results from UMD-2

UMD-2					
	Average Bulk Density	Avg. Dry ITT (psi)	Number of Specimens	Standard Deviation	Variance
In-situ Pavement	2.38	147.1	3	40.9	1670
Heated in-situ Pavement	Na	133.9	3	17.9	319.8
New Patch	2.14	104.5	3	2.7	7.3

The results from the asphalt core testing represent a relative comparison between the in-situ pavements at the sites and the patch material. It is intrinsic that the repaired patch will be more durable and stronger than the damaged pavement but it

would be desirable for the patch to equal or exceed the properties of the surrounding in-situ pavement. It is important to keep in mind that there are a number of uncertainties that are uncontrolled in these experiments, most importantly the aggregate gradation and binder of the in-situ section pavements and the new HMA and the age of the in-situ pavement. However these tests reveal several important things about the current repair process and allow reasonable inferences about potential improvements.

Notably it is seen that the IAR repair process produces patches that are below the strength of the in-situ pavement. Investigating this further it was found that in all three test sites in Phase-1, the mean between the dry tensile strengths of the in-situ cores and the patch cores were significantly different per Student T-testing with p=0.10. However it is important to note that the bond interface of the patch assessed at the joint at UMD-1, up until now only anecdotally reported as good (Freeman and Epps, 2012), was found to have excellent tensile strength, rivaling that of the parent material. Figure 23 shows how the joint specimens were tested for tensile strength.

Figure 23 Indirect tensile testing setup. Specifically shown is the testing setup for assessing the thermal bonding of the patch joint.

A full depth saw-cut patch was performed to compare the infrared patches to more conventional pavement repair techniques. This consisted of using a masonry saw to cut through 4 inches of asphalt pavement to the base. A tack coat was then applied and two 2 inch lifts were compacted into the patch. Comparing the infrared repair patches with this conventional full depth saw-cut patch, it was also determined that the mean tensile strength of the infrared patch was below that of the full depth saw-cut patch (Student T-test, $p=0.10$).

The bulk specific gravities of the materials offer a possible explanation for the differences in tensile strength. Compaction for all patches was performed with a Vibco® GR-3200 1.5 ton vibratory compactor. There is currently no recommended compaction quality control for IAR patching besides the standard practice of starting compaction at the patch edges, leveling to grade, and ensuring that the HMA does not fall below acceptable temperatures. In fact during compaction asphalt shoving was observed during the test at UMD-1. What was readily apparent from the laboratory results is that the bulk specific gravities of the asphalt cores from the in situ-existing pavement are all significantly higher than those of the IAR patches. The bulk specific gravity of the saw-cut patch falls between the two. Of note is that the 9 month old IAR patch had a higher bulk specific gravity and tensile strengths than the all of the newer patches except UMD-1, suggesting that the traffic loading it sustained leads to improved densification over time.

These results provided guidance for the Phase 2 testing in the project. The main properties to be investigated were patch density, the rate of rejuvenator application, asphalt tensile strength, and the potential for asphalt charring. Assessment of the patch

material's stiffness and rutting potential via testing and analysis of dynamic or resilient modulus of the patch material was deemed to be beyond the scope of this study but has been addressed by the Army Corp of Engineers in their publication (Carruth & Mejías-Santiago, et al 2014).

For Phase 2 testing, nine patches were performed on the University of Maryland campus. They are indicated as UMD-3 with patches I, II, III, IV, V, VI, VII, VIII, and IX. Patch I is a patch performed per usual by the work crew in accordance with their usual methods. Patch II used 1.5 times the typical compactive effort of a repair, which usually is 20 passes with the Vibco-3200 roller. Patches III and IV utilized the two stage heating approach developed from the finite difference model. Patches V thru IX varied the amount of asphalt rejuvenator applied, ranging from 0-3% by weight of material.

6.1.1 Density

Density has historically been an important marker for QA/QC of asphalt construction. It is fairly easy to assess and a commonly used metric in the industry. This study choose to assess the density of the patch material in relation to the density of the existing pavement residing next to the patch. This relative comparison is useful as the undamaged existing pavement should act as a baseline to compare the patch materials properties and overall quality. Density was assessed in two ways for this study. One was a traditional approach following ASTM D2726 *Standard Test Method for Bulk Specific Gravity and Density of Non-absorptive Compacted Bituminous*

Mixtures and the other was via a non-nuclear density gauge supplied by Troxler Laboratories.

6.1.2 Rejuvenator Application

The IAR patching method requires some percentage of virgin HMA, asphalt rejuvenator, or a combination of the two. The effect of rejuvenator application rate on the density and tensile strength of the patches was therefore investigated. The dosages of Cyclogen rejuvenator were based upon the work of the USACE (Carruth & Mejías-Santiago, et al 2014), which investigated percentages by weight ranging between 1-2.5%. A fan spray applicator was used in the present study. This applicator had a measured flow rate of roughly .0625 gallons/15 seconds. Patches V-IX were sprayed for 0, 15, 30, 45, and 60 seconds respectively. The percent application by weight was computed based upon the assumption that the rejuvenator would soak into and permeate the top ½ inch of the exposed heated and scarified surface, Table 14.

Table 14 UMD-3 tests with the amount of applied rejuvenator.

Patch	Time of Spray	Gallons Applied	Area of Patch (SY)	Gal/SY	% by Weight
V	0	0	1.32	0.00	0
VI	15	0.0625	1.31	0.05	0.8
VII	30	0.125	1.25	0.10	1.6
VIII	45	0.1875	1.34	0.14	2.4
IX	60	0.25	1.32	0.19	3

6.1.3 Two Stage Heating Method

The two stage heating method was implemented for two of the nine patches at site UMD-3 (Patch III and IV). The objective of the two stage heating was to increase the depth of heat penetration. The scheme adopted was to heat the pavement initially for the normal length of time, as chosen by the work crew. Then, after scraping off the top ½ inch and scarifying the new surface, the patch is heated again until it reached 350º F, which was designated as a cutoff point due to concerns about charring. At that point the patch would proceed as normal with the application of rejuvenator, addition of HMA, luting, and compaction.

Patch III was heated initially for 8 minutes, which brought the surface temperature to a maximum of 439ºF. At that point the heater was taken off the patch and it was allowed to cool for 7 minutes to 150ºF before the heater was reapplied for 7 minutes, bringing the surface temperature to 350ºF.

Patch IV was heated initially for 12 minutes, which brought the surface temperature to a maximum of 451ºF. At that point the heater was taken off the patch and it was allowed to cool for 3 minutes to 100ºF before the heater was reapplied for 3 minutes, bringing the surface temperature to 405 F.

Unfortunately because of the scarification the embedded thermocouples could not stay in the asphalt mat to measure the heating caused by the reheating process. The surface probe was maintained on the surface and was functional. The scenario from Patch IV is presented below in Figure 24.

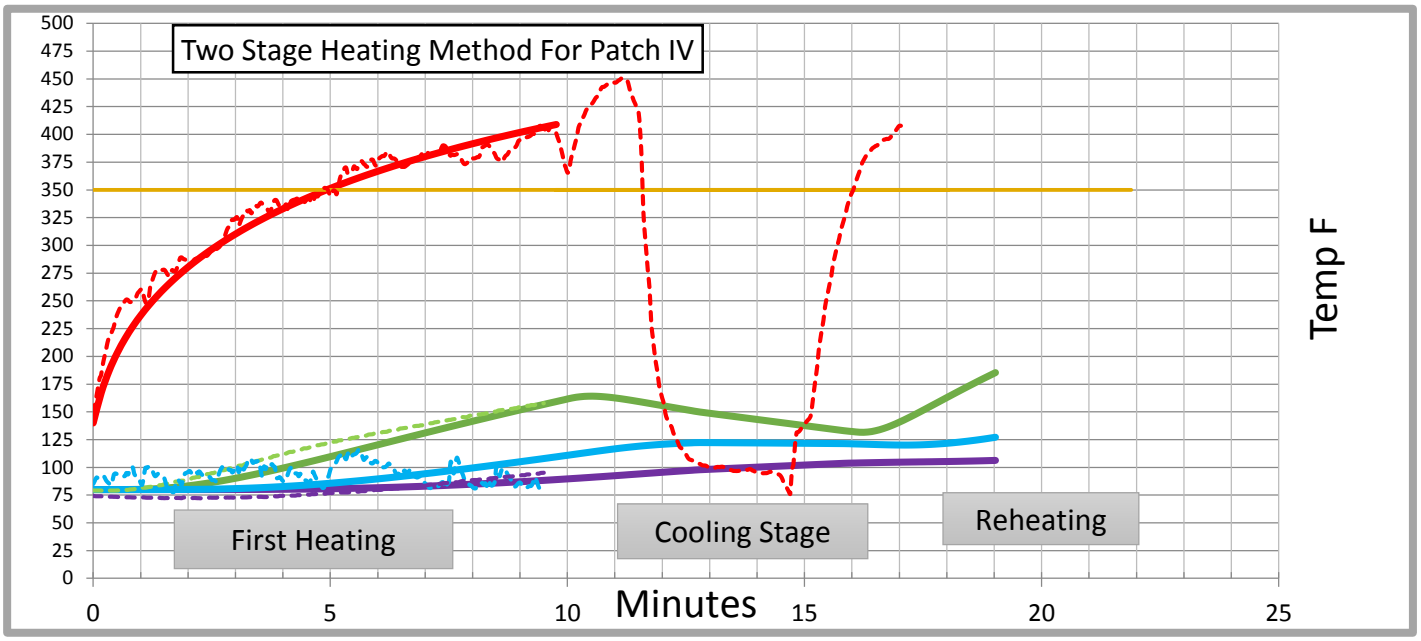

Figure 24 Shown is the two-stage heating process as measured in UMD-3 test IV. Measured temperature is represented by the dotted lines and predicted temperatures by the solid.

6.2 Field Evaluation of Patch Density with Troxler Non-Nuclear Density Gage

The Troxler PaveTracker Plus non-nuclear density gauge provides a quick and easy way to assess the density of an IAR patch. Outside of research studies, coring is an impractical approach for assessing asphalt patch density. Nuclear density gauges, used effectively on large projects, have the disadvantage of strict licensing and usage

procedures. Other non-nuclear density gages are available on the market such as the Trans Tech Pavement Quality Indicator (PQI), but they were not assessed in this study.

6.2.1 Troxler Non-Nuclear Density Gage

The PaveTracker, seen in Figure 25, is a light weight nonnuclear device for measuring the bulk density of an HMA mixture. As the asphalt is compacted and air voids are reduced, these gauges measure the increase in density rather than the absolute material density. The device measures changes in electric fields that result from the introduction of a nonconductive (dielectric) material (i.e., HMA). The device measures bulk density through an electrical field that responds to changes in electrical impedance of the material which, in turn, is a function of the composite resistivity and dielectric constant of the material being measured. (Kvasnak et al, 2007).

Whenever an electrical charge is applied to a conductor, an electrical field is produced. If a dielectric is introduced into this electric field, the strength of the field is reduced. The amount by which this dielectric reduces the electrical field can be characterized by the dielectric constant, a material property. Each component of asphalt concrete—the asphalt binder, aggregates, air, and moisture—has a different dielectric constant. A measurement should first be taken on an asphalt concrete sample of known density. As the asphalt concrete is compacted and air voids decrease, the change in the measured dielectric constant can be related to density.

Aggregate type, binder type, and mixture volumetrics all influence the value of the dielectric constant. If the non-nuclear density gauge is not calibrated to the specific

asphalt mix under investigation then only relative comparisons can be made. This allows these devices to be effective tools for quality control but with more limited utility for quality assurance as the device would need to be calibrated to the density obtained from cores.

The Pave Tracker Plus measurements are almost instantaneous when the device is placed on the surface of an asphalt mat. It has an adjustable depth of measurement, which for this study was set to 2 inches. Areas of segregation, lower density levels along longitudinal joints, or other non-uniform areas can be detected by the PaveTracker Plus, which allows the operator to correct the problem before construction is complete. The PaveTracker can be used exactly like the nuclear density gauge but without the use of any nuclear material. The PaveTracker also has an onboard real-time recording system for the density values.

Figure 25 Troxler Pave Tracker Plus in use by the author.

6.2.2 Results with the Density Gage

Results from using the Troxler Pave Tracker are shown in Figure 26 and Table 15. The results generally show that immediately after compaction the average density reading from the gage is overestimated by the Pave Tracker gauge by a margin greater than 5% of the measured density from the sampled cores. Interestingly when the patches were measured again a week later it was found that the Pave Tracker generally estimated the patch density within a 5% margin of the measured densities from cores. The reason for this effect is suspected to be the moisture content in the fresh HMA. Steaming was observed from the freshly laid and compacted HMA and, as discussed above, the presence of water can affect the density readings taken from non-nuclear density devices.

Interestingly, if only the subset of results from tests UMD-3-V thru UMD-3-IX are examined there is a general trend that as the rejuvenator dosage (which is a 1:1 ratio of water and the concentrated maltenes slurry) increases from test V-IX, the immediately measured densities increase, with V having the lowest measurement of all. Patch IX represents an outlier to this trend. Tests I-IV, as would be expected have fairly similar immediately measured densities due to their fairly consistent rejuvenator application rates.

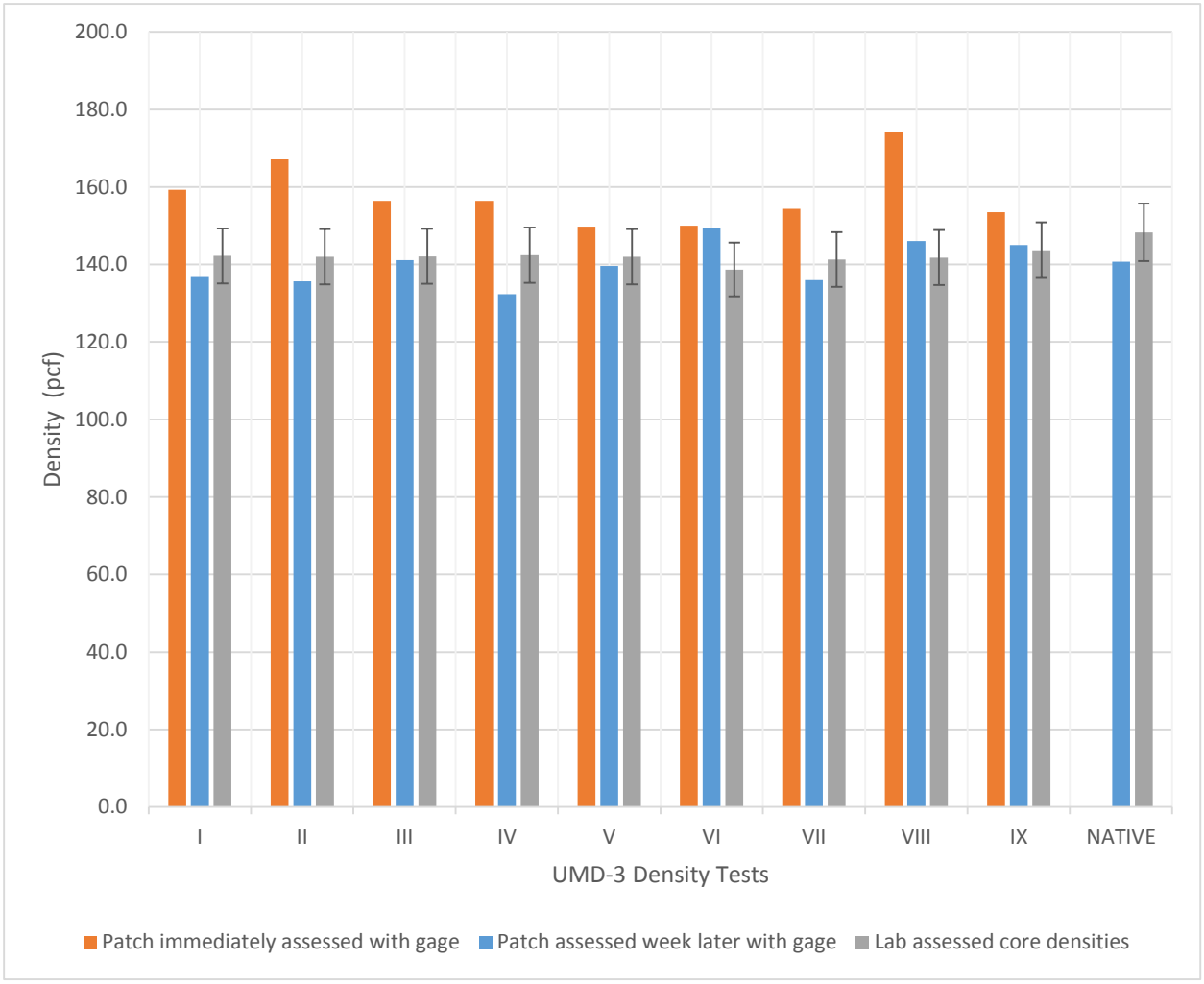

Figure 26 Results of the Troxler Density gauge with a 5% tolerance with respect to the lab assessed densities.

Table 15 Compilation of Test Site Density Metrics

Location	Temperature During Compaction (F)	# of passes	**Gauge Measured Density After Compaction (pcf)**	St. Dev.	Var.	**Gauge Measured Density Week Later (pcf)**	St. Dev.	Var.	**Average Density from Cores (pcf)**
UMD-1	198.5	-	-	-	-	**141.525**	7.7	59.4	**146.0**
UMD-1-Existing Pavement	-	-	-	-	-	**131.2**	5.3	28.3	**151.0**
UMD-2	-	-	-	-	-	**155.65**	10.9	117.7	**133.5**
UMD-2-Existing Pavement	-	-	-	-	-	**141.8**	8.2	68.0	**148.5**
Waldorf-Saw cut	226.4	20-two lifts	-	-	-	-	-	-	**142.9**
Waldorf-Old Patch	-	-	-	-	-	-	-	-	**139.8**
Waldorf-New Patch	198.5	-	-	-	-	-	-	-	**137.3**
Waldorf-Existing Pavement	-	-	-	-	-	-	-	-	**142.9**
UMD-3-I	230.7	21	**159.3**	3.2	10.2	**136.7**	3.6	12.9	**142.2**
UMD-3-II	226.0	31	**167.2**	2.8	7.7	**135.7**	12.9	166.6	**142**
UMD-3-III	235.0	29	**156.4**	3.6	13.0	**141.1**	4.9	23.7	**142.1**
UMD-3-IV	234.3	25	**156.4**	8.1	65.2	**132.3**	7.3	53.8	**142.4**
UMD-3-V	215.2	20	**149.8**	1.8	3.3	**139.6**	8.6	73.3	**142**
UMD-3-VI	208.0	18	**150.0**	7.6	57.2	**149.5**	6.5	42.3	**138.7**
UMD-3-VII	250.5	19	**154.4**	4.8	23.1	**136.0**	19.6	382.9	**141.3**
UMD-3-VIII	212.7	28	**174.2**	5.6	30.9	**146.0**	7.7	59.5	**141.8**
UMD-3-IX	257.4	21	**153.5**	8.3	68.3	**145.0**	9.6	91.7	**143.7**
UMD-3-Existing Pavement	-	-	**142.6**	-	-	**140.8**	9.5	90.7	**148.3**

6.3 Laboratory Analysis-Phase-2 Testing

The laboratory results for bulk specific gravity and indirect tensile (IDT) strength measured in accordance with ASTM D6931 *Standard Test Method for Indirect Tensile (IDT) Strength of Bituminous Mixtures* from the Phase 2 testing at the UMD-3 site are presented in Table 16. What is clearly evident is the relationship between the bulk density and the average indirect tensile strength, both wet and dry, as can be seen clearly in Figure 27. However it is important to recognize that the additional passes that were performed for Patch II, 31 rather than 20, seemed to have no impact on the density of the material and in fact there seems to be an upper bound of 2.28 for the densities of the patches. This implies that additional passes may have little impact on density unless a larger vibratory compactor is used.

A significant finding is that, for the same average bulk densities, the patches that underwent the two stage heating process had remarkably better performance in terms of dry IDT strength and Tensile Strength Ratio (TSR). There also appears to be a slight correlation between the dosage of asphalt rejuvenator and TSR values when patches V thru IX are examined, Figure 28. This data however contains a great deal of noise since the densities of Patches V-IX varies from 2.22 to 2.30, unlike those of Patches I-IV which conveniently had consistent densities of 2.28. As such, an analysis was done to correct the wet and dry tensile strengths of Patches V-IX using the results from Figure 27. Patches V-IX were assigned a pseudo-density of 2.28 and the density corrected data is also presented in Figure 28 as the density corrected data. This shows a better correlation with an increase in rejuvenator application to the increased

durability of the patch as measured by tensile strength ratio (TSR). Importantly this apparent increase in the TSR is a result of a decrease in the dry indirect tensile strength, this effect can be seen in Figure 29 when looking at the density corrected data. The main take away from this is that the dry IDT strength decreases as the rejuvenator dosage increases but the wet IDT remains the same. This is likely due to the material softening as more rejuvenator is added. Not accounted for is the amount of virgin HMA that was used for each patch.

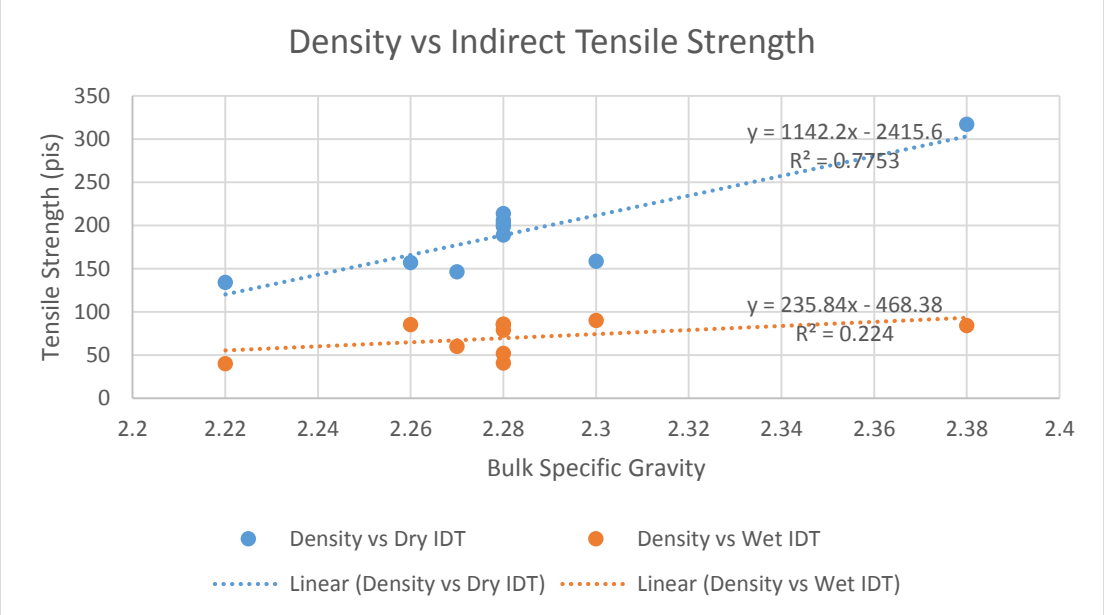

Figure 27 Density compared to indirect tensile strength

Table 16 Summary of Results from UMD-3

UMD-3 Site					
			IDT Testing (PSI)		
Location	Specimen	Bulk Specific Gravity	Dry IDT	Wet IDT	
Native Pavement	Nat-1	2.39		54.41	
	Nat-2	2.38	256.78		
	Nat-3	2.38	369.99		
	Nat-4	2.39		73.84	
	Nat-5	2.36	324.21		
	Nat-6	2.36		123.53	**TSR**
	Average	**2.38**	**316.99**	**83.93**	**0.26**
	St Dev	0.01	56.95	35.65	
	Var	0.00	3242.80	1271.02	
I-Normal Patch	I-1	2.22		33.55	
	I-2	2.29	206.16		
	I-3	2.26	191.48		
	I-4	2.30	219.76		
	I-5	2.25		14.84	
	I-6	2.34		73.64	**TSR**
	Average	**2.28**	**205.80**	**40.68**	**0.20**
	St Dev	0.04	14.14	13.22	
	Var	0.00	199.91	174.88	
II-Heavy Compaction	II-1	2.26		38.84	
	II-2	2.25	215.16		
	II-3	2.25		48.26	
	II-4	2.29	193.46		
	II-5	2.31		68.24	
	II-6	2.30	188.07		**TSR**
	Average	**2.28**	**198.90**	**51.78**	**0.26**
	St Dev	0.03	14.34	15.01	
	Var	0.00	205.66	225.30	

Table 16 Continued

UMD-3 Site					
			IDT Testing (PSI)		
Location	Specimen	Bulk Specific Gravity	Dry IDT	Wet IDT	
III-Two Stage Heating	III-1	2.25	221.94		
	III-2	2.31		110.22	
	III-3	2.27		60.76	
	III-4	2.31	186.60		
	III-5	2.26		NA	
	III-6	2.28	203.71		
	III-7	2.26	143.00		**TSR**
	Average	**2.28**	**188.81**	**85.49**	**0.45**
	St Dev	0.02	33.78	34.97	
	Var	0.00	1140.93	1222.85	
IV-Two Stage Heating	IV-1	2.31		91.65	
	IV-2	2.29		78.85	
	IV-3	2.32	247.32		
	IV-4	2.19	126.84		
	IV-5	2.31	231.84		
	IV-6	2.27		NA	**TSR**
	Average	**2.28**	**202.00**	**85.25**	**0.42**
	St Dev	0.05	65.55	9.05	
	Var	0.00	4296.73	81.93	

Table 16 Continued

UMD-3 Site					
			IDT Testing (PSI)		
Location	Specimen	Bulk Specific Gravity	Dry IDT	Wet IDT	
V-0% rejuvenator	V-1	2.26		63.48	
	V-2	2.28	218.85		
	V-3	2.27		87.77	
	V-4	2.30		85.49	
	V-5	2.29	231.29		
	V-6	2.25	190.64		**TSR**
	Average	**2.28**	**213.59**	**78.91**	**0.37**
	St Dev	0.02	20.83	13.41	
	Var	0.00	433.86	179.89	
VI-0.8% rejuvenator	VI-1	2.23		39.57	
	VI-2	2.23	172.81		
	VI-3	2.23		NA	
	VI-4	2.30		39.88	
	VI-5	2.23	150.63		
	VI-6	2.13	93.55		
	VI-7	2.20	118.71		**TSR**
	Average	**2.22**	**133.92**	**39.72**	**0.30**
	St Dev	0.05	15.68	0.22	
	Var	0.00	245.93	0.05	
VII-1.6% rejuvenator	VII-1	2.27		96.03	
	VII-2	2.22	184.21		
	VII-3	2.27		80.25	
	VII-4	2.22	162.79		
	VII-5	2.31	135.54		
	VII-6	2.29	145.09		
	VII-7	2.28		79.25	**TSR**
	Average	**2.26**	**156.91**	**85.18**	**0.54**
	St Dev	0.03	21.42	11.16	
	Var	0.00	458.83	124.47	

Table 16 Continued

UMD-3 Site					
			IDT Testing (PSI)		
Location	Specimen	Bulk Specific Gravity	Dry IDT	Wet IDT	
VIII-2.4% rejuvenator	VIII-1	2.34	200.64		
	VIII-2	2.29		NA	
	VIII-3	2.26		59.76	
	VIII-4	2.28		NA	
	VIII-5	2.29	158.60		
	VIII-6	2.21	111.22		
	VIII-7	2.23	114.23		**TSR**
	Average	**2.27**	**146.17**	**59.76**	**0.41**
	St Dev	0.04	42.28	-	
	Var	0.00	1787.50	-	
IX-3% rejuvenator	IX-1	2.33		75.05	
	IX-2	2.37	193.91		
	IX-3	2.33		130.42	
	IX-4	2.29		63.68	
	IX-5	2.21	125.02		
	IX-6	2.28	156.17		**TSR**
	Average	**2.30**	**158.37**	**89.72**	**0.57**
	St Dev	0.06	34.50	35.71	
	Var	0.00	1190.34	1274.91	

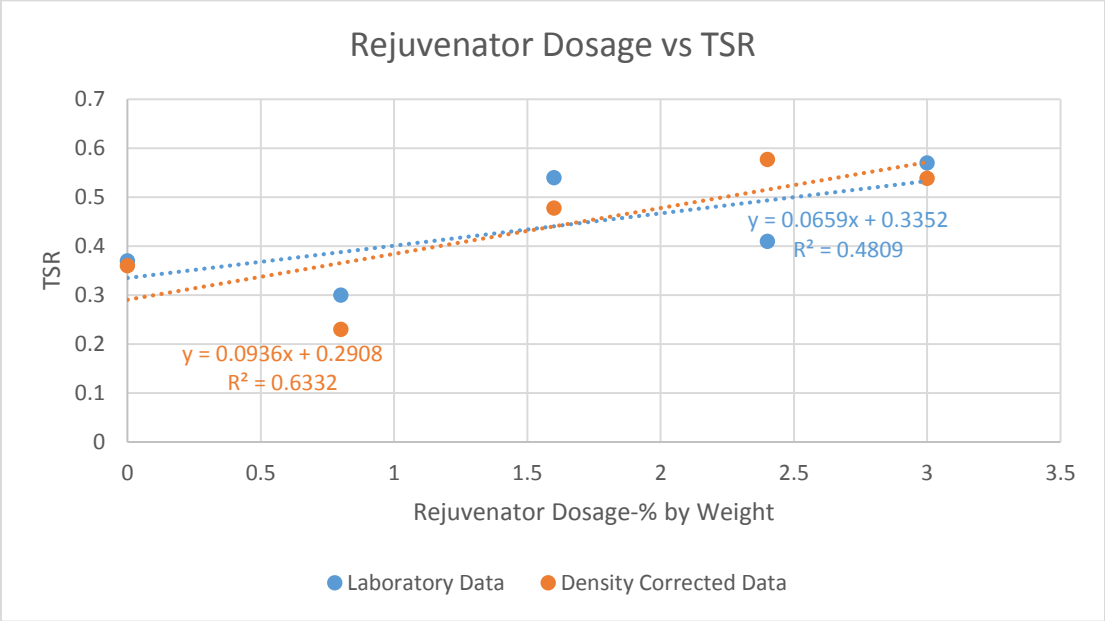

Figure 28 Rejuvenator dosage compared with tensile strength ratio

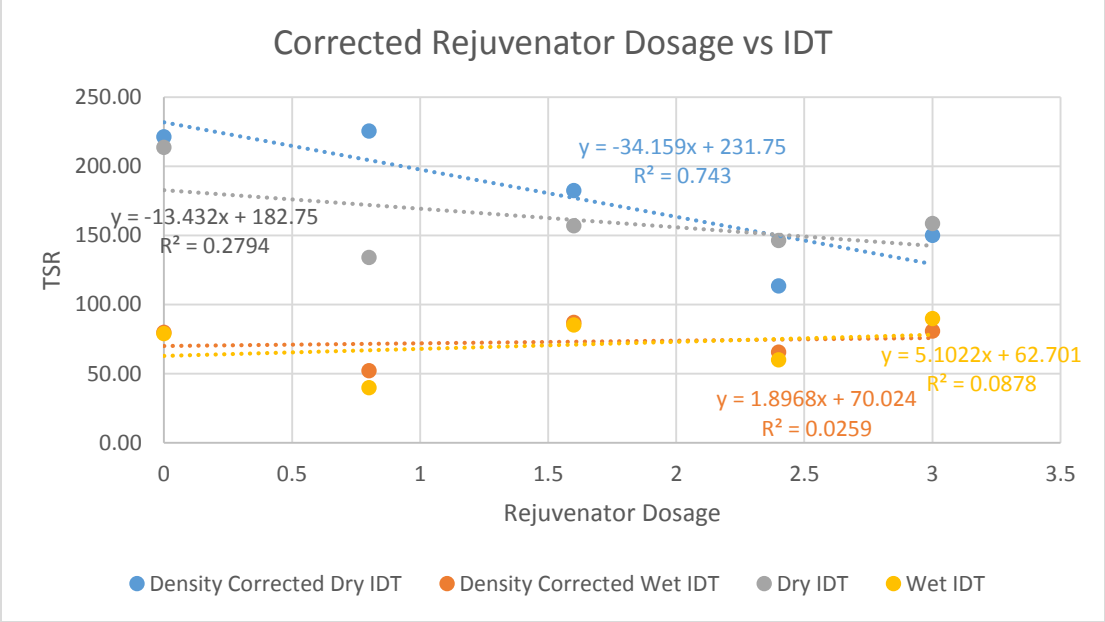

Figure 29 Rejuvenator application compared to indirect tensile strength.

6.4 Conclusions

The most significant findings of this study relate to the effects of density, rejuvenator application, and heating methods. As may be imagined from typical asphalt projects, density has a large impact on the quality of the IAR patch materials. Proper densification directly impacts the tensile strength of the patch material and the raveling potential as expressed by the TSR. The compaction process as measured throughout the testing at UMD-3 showed that the asphalt temperatures during compaction were all in acceptable ranges (Table 15) and the laboratory results from Patch II show that no appreciable increase in density is seen as more passes are applied. What is suggested as a result of this study is the adoption of a larger compactive device.

Rejuvenator dosage had a minimal if not negligible effect on the density of the asphalt patch. However there is a correlation between the rejuvenator application and the tensile strength. Though this is not readily apparent until the results from the patches have been corrected for density, Figure 28 & 29, rejuvenator dosage seems to have a significant influence on the dry tensile strengths. As more rejuvenator is added the dry tensile strength decreases while the wet tensile strength remains relatively constant. This increases the TSR. This trend is likely due to material softening as the amount of maltenes increase within the pavement. This is not necessarily a bad trend as, with an increase in rejuvenator, the dry and wet behavior of the patch material become more consistent. Large variations in the dry and wet behavior can be undesirable.

It is suggested that future research be performed on the rutting potential as a function of rejuvenator dosage via resilient modulus and/or repeated load permanent

deformation testing. Due to the inconclusive nature of these results it is suggested that the dosage rate of around 1.5% rejuvenator by weight of mix as suggested by the USACE be adopted to balance the stiffness and rutting resistance of the patch. This value is also within the bounds of acceptable rejuvenator application reported by the Basic Asphalt Recycling Manual (FHWA, 2001).

The use of the two stage heating technique at the UMD-3 site for Patches III and IV was deemed successful as it resulted in an increase of the measured TSR. This would seems to indicate the potential for better thermal bonding along the bottom of the patch where the new HMA interfaces with the existing material. The data from the Phase-1 testing at UMD-1 seems to confirm the anecdotal analysis of others (Uzarowski et al, 2011) that for IAR patches the surface joint along the sides of the patch and the existing pavement is strong and the IAR process in general seems to minimize the potential of cold joints. The data from this study indicates that the increased depth of heat penetration predicted in Figure 24 from two-stage heating method can allow for better bonding with the underlying material and a more durable patch.

On the whole the patching performed in the manner described in this study is successful when based upon a relative strength criteria to the surrounding pavement. The data from Tables 11-13 and Table 16 show that that the patch material can have a density within 3-10% of the in-situ pavements density, wet indirect tensile strength on par with the surrounding pavement, dry tensile strengths that are at least half of that of the in-situ pavement, and resulting TSR's that are superior to those of the in-situ

pavement. In addition result Tables 12 and 13 indicate that the surrounding pavement that may be heated during the repair process are not harmed and retain their strength.

Most intriguing perhaps is the potential application of non-nuclear density gages for quickly and easily assessing the density of the patch relative to the existing pavement surrounding the patch. Based upon the data from this study shown in Figure 25, there is certainly potential to use these devices as a means to ensure post project quality control. However issues with moisture sensitivity may limit their application for immediate assessment of IAR patches that are still hot and steaming. If a multiple patches are performed at the same site (as is often the case with potholes and cracking) there is good potential that the crew using the device can come back through the project site before leaving and use the non-nuclear gage to assess the quality of their work.

Chapter 7: Conclusions and Lessons Learned

7.1 Application of Results

The importance of proper compaction, rejuvenator application, and heating techniques have been shown in this work. Achieving proper density is key to ensuring patch strength, along with balancing the strength and stiffness requirement of the patch via rejuvenator application, and managing temperatures within the heated asphalt mat in order to ensure better durability. These results from this study are to be used in the development of a set of construction specifications to provide guidance to those in the asphalt recycling industry. Specifications are critical to adoption of infrared heating repair as an approved process by local, county, and state agencies. Many agencies and institutions have resource and other that make it unlikely that they will develop these specifications internally. Consequently, a major deliverable from this study is a model specification having a solid technical foundation that agencies can either adopt outright or conveniently adapt to their own particular needs. This is especially important because there are several different commercially available IAR methods such as the HeatWurx method and the Pothole Pro method that can have drastically different results.

7.1.1 Important Factors in Successful Infrared Patching

Key factors in the IAR process have been identified by this study and addressed in the construction specification. In summary, they include the following:

Material requirements

- Recycling agent type, source, and application rate
- Aggregate source and gradation
- Asphalt cement source and grade
- Admixtures

Equipment requirements

- Age or operating condition of the equipment
- Types and numbers of heating units and heating fuel
- Emission controls
- Type of scarification
- Method, control, and accuracy of recycling agent addition
- Blending and uniformity of the recycled mix
- Type of spreading and leveling equipment
- Type of compaction equipment

Construction methods

- Pavement surface preparation prior to repair
- Pre-heating dimensions
- Minimum and maximum pavement surface temperature prior to scarification/rotary milling
- Depth of heating
- Number and type of rollers required for compaction
- Weather conditions at the time of HIR construction

Inspection and QC/QA

Acceptance requirements

- Treatment depth
- Percent compaction
- Smoothness
- Workmanship
- Obvious defects

Measurement and payment

- Square yard

Special provisions

- Limits of work
- Construction schedule, staging, or limitations on hours of work
- Trucking requirements
- Traffic accommodation requirements
- Existing roadway material properties
- Mix design information
- Any other site-specific requirements

7.1.2 Quality Assurance and Quality Control Specifications Developed

The Quality Control Specification developed in this study is based primarily on existing specifications from the AASHTO Technology Implementation Group and the results of best practices established by this study and others. The draft specification is

included as Appendix A. In addition, during the course of this study it was found that the importance of keeping good project records cannot be understated. A short one page document has been developed to record salient project details in an effort to increase adherence to best construction practices. The document also acts as a record for both the contractor and the owner in order to ensure that proper QA/QC procedures were followed during construction. This is particularly important in case a premature patch failure occurs.

7.2 Lessons Learned and Future Work

This project has addressed a number of issues regarding Infrared Asphalt Repair methods. It is hoped that the proposed construction specification will be adopted and then modified by others as more details about this process become clearer and more field data becomes available. Some additional important issues were also identified that could be pursued in future work:

- *Assessment of Compactive Effort.* The compactive effort applied by other commercially available compaction machines, such as steel drum rollers and larger vibratory rollers, should be evaluated to determine whether higher densities are achievable.
- *Proportions of old vs. new material*. The current proportioning method is largely qualitative, although it seems to work. Field trials should be used to evaluate the effect of varying the proportion of new material. It could be the case that the

addition of larger quantities of new virgin HMA has a larger impact than rejuvenator application dosages.

- *Field mixing*. In the current process, the new HMA mixture is worked into the upper portion of the scarified existing material using a rake. The control of this process to ensure satisfactory mixing is purely qualitative—i.e., the mixture is raked until it "looks right." Some method for standardizing this should be developed and included in the specification.
- *Resilient modulus testing*. Cores from within and outside the patch should be tested to determine if they have comparable stiffness. The portion of virgin HMA to old material and the dosage of asphalt rejuvenator will undoubtedly have an impact on these results.
- *Repeated load permanent deformation testing.* Cores from within and outside the patch should be tested to determine if they have comparable rutting resistance. The portion of virgin HMA to old material and the dosage of asphalt rejuvenator will undoubtedly have an impact on these results.

Appendix A: Proposed QA/QC Contract Documents

QA/QC PROJECT REPORT

GENERAL INFORMATION

Date:_____ Location:_____

Property Owner:_____ Foreman on Site: _____

Air Temperature:_____ Weather (i.e. Wind, Rain, Sunny):_____

Additional Notes:_____

MATERIAL INFORMATION

HMA

Asphalt Plant:_____

Time of Pickup:_____

Initial Temp (F) :_____

HMA Binder:_____

HMA Gradation:_____

Asphalt Rejuvenator

Product Name:_____

Water Ratio:_____

Amount Applied:

Patch 1:_____(gal)

Patch 2:_____(gal)

Temperature of HMA in Hotbox:

Time:							
Temp:							

Additional Notes:_____

SITE INFORMATION

Number of Patches:_____ (See Back for Additional)

Patch ID	Issue (i.e. crack, pothole)	Depth to Issue	Patch Square Footage
1			
2			

Additional Notes:_____

HEATING INFORMATION

Pavement Temp. After Heating:_____ Duration of Heating:_____

Temp. During Compaction:_____ Temp. At Opening To Traffic:_____

Additional Notes:_____

COMPACTION INFORMATION

Roller Used:_____ Number of Lifts:_____ Number of Passes per Lift:_____

Native Pavement Density:_____ Patch Densities:_____

Additional Notes:_____

Maintenance Specification

INFRARED BITUMINOUS SEAMLESS PAVEMENT REPAIR

PART 1 GENERAL

1.1 SECTION INCLUDES

A. Products, procedures and equipment to provide a seamless repair of bituminous pavement by the application of evenly distributed infrared heat to aid in the reworking and remixing of the existing asphalt mix.

1.2 RELATED SECTIONS

A. Specific related sections shall be mandated by the Owner or Local Municipal Authority.

1.3 REFERENCES

A. American Association of State Highway and Transportation Officials
   1. Maintenance Specification Section 00856 Infrared Bituminous Seamless Pavement Repair
   2. AASHTO M140
   3. AASHTO M208

B. Canon City, Colorado-Department of Public Works
   1. Maintenance Specification Section 02740 Flexible Pavement

C. Somerset County, New Jersey-Department of Public Works
   1. Specifications and Fee Schedules for Road Openings

D. American Society for Testing and Materials
   1. ASTM D4552

1.4 DEFINITIONS

A. Owner-agent: individual or department who is contracting out the work for the pavement repairs

B. Contractor-agent: company or individual who has the contract to perform said pavement repair work

C. Virgin HMA: Virgin Hot Mix Asphalt picked up from an asphalt plant

D. Hotbox: temperature controlled container for transporting HMA at its required temperature

1.5 SUBMITTALS

A. Provide manufacturer's product data, equipment specifications and material specifications as part of the bid package. Failure to do so will constitute a non-responsive bid and the bid will be rejected.

1.6 ACCEPTANCE

A. Repair area to match existing grade, be tightly compacted, have a skid resistant surface, and tightly bonded to the existing adjacent pavement. The patch should provide a seamless transition to the surrounding undamaged pavement.

1.7 MEASUREMENT

A. Square foot of the accepted repaired area at the measured depth of repair.

1.8 PAYMENT

A. Accepted repaired quantities paid for at the contract unit price per square foot at the measured depth of repair OR per agreement between the Contractor and Owner.

PART 2 PRODUCTS AND EQUIPMENT

2.1 MATERIALS

A. Hot Mix Asphalt Pavement (HMA) uniformly mixed and well graded. Superpave binder grade will be specified by the Owner OR the Contractor will maintain records to be given to the Owner at the completion of the work of the plant that supplied the HMA and of the gradation and Superpave binder grade that is utilized in the Infrared Pavement Repair process.

1. Aggregate size for Wearing Course is recommended as 9.5mm maximum, well-graded aggregate.
2. From pick up through placement the Contractor will conduct and record periodic temperature checks of the Virgin HMA in its hotbox to ensure the temperature does not fall below 250ºF or exceed 300ºF. This documentation will be provided to the Owner at the completion of the work.

B. Asphalt Rejuvenator Agent (ARA) shall be a petroleum product additive that falls under the one of the recycling agent (RA) groups outlined in ASTM D4552

C. Tack Coat/Sealant shall be emulsified asphalt with the same asphaltic cement as the HMA pavement mix placed, SSI or equal. In accordance with requirements of AASHTO M140 or M208

2.2 EQUIPMENT

A. Pavement Restoration Vehicle (PRV) shall be a truck mounted, self-contained pavement maintenance heating system (Hotbox) equipped with a fuel system and a heated chamber capable of maintaining the fresh asphalt at a temperature of 250-300ºF.

B. The adjustable height infrared heating unit may be truck or trailer mounted to the PRV. The unit shall be equipped with a chamber or chambers capable of heating the existing bituminous pavement to a workable condition without oxidation or burning. There shall be no flame in direct contact with the existing bituminous surface.

C. The sprayer for the asphalt rejuvenator agent (ARA) shall deliver the ARA with a fan spray ensuring equal and uniform coverage of the heated. The sprayer shall have a clear tank with measurement markings on the side or a fluid gauge to determine the amount of ARA used.

D. Compaction shall be achieved with a self-propelled vibratory steel drum roller.

PART 3 EXECUTION

3.1 MARK AND MEASURE REPAIR AREA

A. Identify, mark and measure the specific area to be repaired in coordination with the Owner's representative.

3.2 ENVIRONMENTAL REQUIRMENTS

A. The Contractor shall ensure that asphalt is not placed in the rain or in wet conditions. In high wind conditions a metal wind shield that extends ¾ the way around the outside of the heater is to be used to minimize convective heat losses.

3.2 CLEAN REPAIR AREA

A. Thoroughly sweep, air blow, or hose the general area to be repaired to remove dirt and debris.

3.3 CONSTRUCTION

A. The Contractor and Owner will clearly define in the bid submittal or contract the extent of required traffic control and the party responsible for providing traffic control for the site.

B. Heat area to be repaired to a sufficient temperature using infrared heat to allow remixing of the asphalt without oxidation or burning.
   1. The heater shall be lowered to within 10-14 inches of the existing pavement, centered over the damaged area.
   2. Do not exceed a surface temperature of 350º F. Measurement will be conducted with a temperature probe or infrared temperature gun provided by the contractor. If the temperature is exceeded addition material will need to be removed.
   3. Heating is sufficient when the existing asphalt can be worked with a rake to a depth of 2 inches.

C. After heating no less than the top ¼ - ½" of asphalt will be removed to take away any charred material. If the surface temperature exceeds 350ºF as mentioned in section 3.3.C.2, another ½" of material will be removed for every 100ºF over.

D. ARA will be uniformly sprayed to the surface of the heated asphalt with a fan nozzle at a rate of 0.1-0.5 gallons per square yard. The color of the ARA will be used to help assess adequate coverage. The amount of ARA used per patch shall be recorded.

E. Using a hand rake or mechanical tiller, scarify and thoroughly mix the repair area to depth of 2 inches. Add additional virgin HMA as necessary.
   1. When placing additional HMA the temperature shall not fall below 225 degrees F during placement. Temperature of placement shall be recorded by the Contractor.

F. Reshape repair area by hand (luting) to match grade of adjacent pavement.

G. Compact the surface with a vibratory steel drum roller. The surface should be smooth, tight, and matching the grade of the adjacent pavement.
   1. The outside perimeter shall be compacted first in order to ensure a full thermal bond with the existing heated pavement.
   2. If greater than 2 inches of asphalt is to be compacted, multiple lifts should be placed and compacted.
   3. If evidence of asphalt shoving occurs during compaction the vibratory compactor shall be operated in static mode or the pavement shall be allowed to cool for a slight amount of time before compaction resumes per Table 1.
   4. The temperature of the asphalt shall not fall below 175 degrees F during compaction. Temperature at compaction shall be recorded by the Contractor.

H. Stone dust or fine sand may be applied to reduce the tackiness of the patch at the Contractor's discretion. Sand should be evenly distributed over the surface to fill small voids and absorb excess sealant if surface sealant is applied.

3.4 WARRANTY AND QUALITY ASSURANCE

A. The patch quality will be assessed via the use of one or more of the following methods per agreement between the Owner and the Contractor:
   1. Nuclear Density gauge.
   2. Non-nuclear Density gage such as a Pavement Quality Indicator (PQI).
   3. Guarantee of repair quality for __ months.
   4. Alternative method agreed upon by both parties.

B. Failure to meet the warranty requirements constitutes a breach of contract

C. Failure is defined as the following:
   1. Greater than 5% cracking in the repaired area within 12 months
   2. Greater than 5% raveling of material from the repaired area within 12 months
   3. Rutting more than 15 mm within 12 months
   4. Not providing a seamless repair

3.5 FINAL CLEAN UP

A. Sweep up and dispose of excess material and debris.

3.6 OPEN TO TRAFFIC

A. Allow the repaired area to cool to 175ºF before opening to traffic. Measurement will be conducted with a temperature probe provided by the contractor.

END OF SECTION

Chapter 9: References

AASHTO Technology Implementation Group. *Maintenance Specification: Section 00856-Infrared Bituminous Seamless Pavement Repair.* American Association of State and Highway Transportation Officials, Washington, DC. 2010

ANSYS Inc. "ANSYS Thermal Analysis Guide Release 5.5"- *Southpointe, 275 Technology Drive, Canonsburg, PA 15317* (1998)

ASTM, *Standard Practice for Classifying Hot-Mix Recycling Agents*. Designation: D4552/D4552M - 09. ASTM International, 2014

ASTM, *Standard Test Method for Bulk Specific Gravity and Density of Non-Absorptive Compacted Bituminous Mixtures*. Designation: D2726/D2726M - 14. ASTM International, 2014.

ASTM, *Standard Test Method for Percent Air Voids in Compacted Dense and Open Bituminous Paving Mixtures*. Designation: D3203/D3203M - 11. ASTM International, 2014.

ASTM, *Standard Test Method for Effect of Moisture on Asphalt Concrete Paving Mixtures*. Designation: D4867/D4867M - 09. ASTM International, 2014.

ASTM, *Standard Test Method for Bulk Specific Gravity and Density of Compacted Bituminous Mixtures Using Automatic Vacuum Sealing Method. Designation*: D6752/D6752M - 11. ASTM International, 2014.

ASTM,*Standard Test Method for Indirect Tensile (IDT) Strength of Bituminous Mixtures*. Designation: D6931 - 12. ASTM International, 2014.

Bergman, T., Lavine, A., Incropera, F. and Dewitt, D. *Fundamentals of Heat and Mass Transfer.* Seventh Edition. ISBN 13 978-0470-50197-9

Boyer, E.R. *Asphalt Rejuvenators, "Fact or Fable."* Asphalt Institute, 2000.

Cañon City, *Flexible Pavement.* Standard Construction Specifications. City of Cañon City, 2008.

Carruth, W. D., and Mejias-Santiago, M. *In-Place Asphalt Recycling for Small Airfield Repairs in Remote Locations*. Prepared for Consideration and Publication at the 94th Annual Meeting of the Transportation Research Board. 2014.

FHWA, *Basic Asphalt Recycling Manual*. Asphalt Recycling and Reclaiming Association, Federal Highway Administration, 2001.

Freeman, T. and Epps, J. *Heatwurx Patching at Two Locations in San Antonio.* The Texas Transportation Institute, The Texas A&M University System, College Station, Texas, 77843. 2012.

Kvasnak, A. Williams, C. Ceylan. H. and Gopalakrishnan, K. *Investigation of Electromagnetic Gauges for Determining In-Place HMA Density.* Center for Transportation Research and Education, Iowa State University, 2711 South Loop Drive, Suite 4700, Ames, IA 50010. 2007.

Labeas, G.N., Watiti, V.B., and Katsiropoulos, V.*Thermomechanical Simulation of Infrared Heating Diaphragm Forming Process for Thermoplastic Parts.* University of Patras. Journal of THERMOPLASTIC COMPOSITE MATERIALS, Vol. 21—July 2008.

Nazzal, M. D., Kim, S., and Abbas, A. R. Evaluation of Winter Pothole Patching Methods. Prepared for The Ohio Department of Transportation, Office of Statewide Planning & Research. 2014.

Nikishkov, G.P. "Programming Finite Elements in Java" Springer Publications. 2010. ISBN 978-1-84882-971-8

NCHRP Report 626. *NDT Technology for Quality Assurance of HMA Pavement Construction.* Transportation Research Board, Washington, DC. 2009.

NCHRP Report 463. *Pavement Patching Practices.* Transportation Research Board, Washington, DC. 2014.

NCHRP Report 626. *Recycling and Reclamation of Asphalt Pavements Using In-Place Methods.* Transportation Research Board, Washington, DC. 2011.

Pfeiffer, G.H.. *Using Radio-Frequency Identification Technology To Measure Asphalt Cooling.* Presented to Graduate School at University of Maryland, College Park, 2010.

Somerset County, *Specifications and Fee Schedules For Road Openings.* The Board of Chosen Freeholders of Somerset County, NJ., Department of Public Works, 2009.

USDOT, *Hot In-Place Asphalt Recycling Application Checklist.* Publication FHWA-IF-06-011. U.S. Department of Transportation, 2005.

Uzarowski, L. Henderson, V. *Innovative Infrared Crack Repair Method.* Transportation Association of Canada, Edmonton, Alberta. 2011.

Yavuzturk, C, and Ksaibati, K. *Assessment of Temperature Fluctuations in Asphalt Pavements Due to Thermal Environmental Conditions Using a Two-Dimensional, Transient Finite Difference Approach.* Department of Civil and Architectural Engineering, University of Wyoming, 2002.